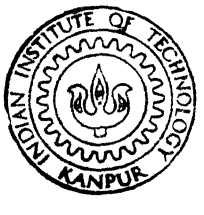
FEM ANALYSIS OF QUASI—STATIC AND ROLLING CONTACT PROBLEMS USING MINIMUM DISSIPATION OF ENERGY PRINCIPLE

by

SURENDRA KUMAR RATHORE

ME
1992
M
RAT
FEM



DEPARTMENT OF MECHANICAL ENGINEERING

INDIAN INSTITUTE OF TECHNOLOGY KANPUR

JANUARY, 1992

FEM ANALYSIS OF QUASI-STATIC AND ROLLING CONTACT PROBLEMS USING MINIMUM DISSIPATION OF ENERGY PRINCIPLE

A Thesis Submitted

in Partial Fulfilment of the Requirements

for the Degree of

MASTER OF TECHNOLOGY

by

SURENDRA KUMAR RATHORE

to the

DEPARTMENT OF MECHANICAL ENGINEERING

INDIAN INSTITUTE OF TECHNOLOGY, KANPUR

JANUARY, 1992

Dedicated

to

My Parents

and

My Nephew ANSHUL

20/1/92

CERTIFICATE

This is to certify that this work on " FEM Analysis of Quasi-Static and Rolling Contact Problems using Minimum Dissipation of Energy Principle " by Surendra Kumar Rathore has been carried out under my supervision and that it has not been submitted elsewhere for a degree.

(Dr. N.N.KISHORE)
Assistant Professor
Department of Mechanical Engineering
Indian Institute of Technology
Kanpur - 208016

January 1992

113078

ME-1992-M-RAT-FEM

w

ACKNOWLEDGEMENTS

I acknowledge with sincerity and deep sense of gratitude, the expert guidance and continuous encouragement provided by Dr. N.N.KISHORE throughout the course of this work.

I highly value the association with my friends Anand, Amul, Saxena, Malhotra and Sood with whom I shared many ideas. I am greatly indebted to Mr. R. C. Mishra for his suggestions and help in the work. I specially thank Mishra Sahib and family for the love and affection extended to me. I am indebted to my wife, Anita for her immense patience and invaluable co-operation. My thanks are due to all my colleagues for valuable suggestions and support during my stay at IITK.

I wish to thank Mr. B. K. Jain for the neat tracing.

I wish to extend my heartiest thanks to faculty members of this institute and Mechanical Deptt. in particular who paved way for me to learn advancement in engineering.

Last, but not least, I feel this my sincere duty to thank the management of Engineering College, Kota for providing me with the opportunity to do this work under QIP.

January, 1992 S.K.Rathore

CONTENTS

Certificate		.. i
Acknowledgement		.. ii
Contents		.. iii
List of symbols		.. iv
List of figures		.. vi
ABSTRACT		..viii
CHAPTER I :	INTRODUCTION	
	1.1 General Introduction	1
	1.2 Literature Survey	3
	1.3 Scope of present work	7
CHAPTER II :	THEORY OF CONTACT PROBLEMS AND MINIMUM DISSIPATION OF ENERGY APPROACH	
	2.1 Basic theory of Contact problem	8
	2.2 Minimum Dissipation of Energy approach	1Ø
CHAPTER III :	FINITE ELEMENT METHOD AND SOLUTION ALGORITHM	
	3.1 Finite Element Formulation	15
	3.2 Contact Conditions	21
	3.3 Application to Quasi-Static Loading	24
	3.4 Application to Rolling Contact	27
	3.5 Implementation Details	3Ø
CHAPTER IV :	RESULTS AND DISCUSSION	
	4.2 Plate with a Hole and Inclusion	35
	4.1 Cylinder Rolling on a Rigid Surface	39
CHAPTER V :	CONCLUSIONS AND SUGGESTIONS FOR FUTURE WORK	68
References		ix
Appendix A		xii
Appendix B		xiv

LIST OF SYMBOLS

l_N	normal clearance
Δl_N	normal clearance change
q_i	external traction components
t	time
u^x, u^y	displacement fields in x & y directions
u_i	displacement components, vector
u_n, u_t	normal and tangential contact displacement vector
x_i, y_i	coordinates of nodal points
D	material property matrix
E	modulus of elasticity
F	nodal force
F_n, F_t	normal and tangential contact nodal force
K's	stiffness matrices
N 's	shape functions
P	load level
ΔP	incremental load step
R, r	radii
S_c	contact boundary
S_t	prescribed traction boundary
S_u	prescribed displacement boundary
T_{pre}	pressure intensity due to precompression
U	nodal displacement
V	volume of domain
X_i	body force components
α_k^i	geometric variable at i^{th} load step
α_n	load incremental ratio

e	penalty term from frictional constraint
ε_{ij}	strain tensor
σ_{ij}	stress tensor
σ_n, σ_t	normal and tangential stresses
σ, ε	stress , strain vector
δ_i	initial clearance
2Δ	area of triangle
Δ	also represents incremental value of parameter
μ	coefficient of friction
ν	Poisson's ratio
τ	tangential stress
Φ_d	dissipation of energy function
Ψ	objective function
Π	potential energy functional
λ	penalty parameter
a,b,c,C	constants
[]	matrix
{ }	vector

LIST OF FIGURES

FIG NO.	DESCRIPTION	PAGE NO
2.1	Schematic representation of a contact problem	13
2.2a	Example contact configuration	14
2.2b	Feasible region	14
3.1	A Representative CST element	32
3.2	Minimisation search algorithm	33
3.3	Different instances of rolling motion	34
3.4	Typical representation of 'n' nodes	34
4.1a	A plate with oversized rigid inclusion	41
4.1b	Representative mesh and prescribed boundary condition	41
4.2	Interface zones while loading in tension from undeformed state (without dissipation),μ=.1	42
4.3	Interface zones while loading in tension from undeformed state (with dissipation),μ=.1	43
4.4	Interface zones while loading in tension from undeformed state (without dissipation),μ=.4	44
4.5	Interface zones while loading in tension from undeformed state (with dissipation),μ=.4	45
4.6	Interface zones while unloading tension (without dissipation) ,μ=.1	46
4.7	Interface zones while unloading tension and loading in compression (with dissipation),μ=.1	47
4.8	Interface zones while unloading tension and loading in compression (without dissipation),μ=.4	48
4.9	Interface zones while unloading tension and loading in compression (with dissipation),μ=.4	49
4.10	Interface zones while unloading compression and loading in tension (without dissipation),μ=.1	50

4.11	Interface zones while unloading compression and loading in tension (with dissipation), μ=.1	51
4.12	Interface zones while unloading compression and loading in tension (without dissipation), μ=.4	52
4.13	Interface zones while unloading compression and loading in tension (with dissipation), μ=.4	53
4.14	Variation of normal stress,at T/Tpre = 0.7	54
4.15	Variation of tangential stress,at T/Tpre = 0.7	55
4.16	Variation of normal stress,at T/Tpre = - 0.7	56
4.17	Variation of tangential stress,at T/Tpre = - 0.7	57
4.18a	Cylinder rolling on rigid surface	58
4.18b	Representative mesh	58
4.19	Effect of friction upon normal force distribution (W/ED = 0.834)	59
4.20	Effect of friction upon tangential contact force distribution (W/ED = 0.834)	60
4.21	Variation of slip and no-slip zones over contact area with friction (at different P/W)(W/ED=0.834)	61
4.22	Distribution of normal force over contact length at differrent P (at constant μ and W)(W/ED=0.834)	62
4.23	Distribution of tangential force over contact length at differrent P (at constant μ and W)(W/ED=0.834)	63
4.24	Distribution of normal contact force at constant P/W and μ (W/ED = 0.834)	64
4.25	Distribution of tangential contact force at constant P/W and μ (W/ED = 0.834)	65
4.26	Variation of energy of dissipation with P/W	66
4.27	Effect of friction upon energy of dissipation at different P/W	67

ABSTRACT

There are many practical situations where two parts are directly in contact subjected to dynamic or varying load. This leads to development of high stresses at contact region and may become a cause of failure. Due to variation in the load, the contact area and contact conditions keep changing and are not known a priori at any load. The problems are non-linear. The regions of slip and no-slip occur at the contact surface. The conditions of contact are determined by the kinematic constraints and Coulomb's law of friction. Finite element analysis of two dimensional elastic quasi-static and rolling contact problems is presented. As the load varies with time, direct application of finite element analysis is difficult as it leads to non-unique solutions if load steps are large and mesh is coarse. In the present analysis, the principle of minimum dissipation of energy is used along with finite element analysis.

The incremental loading and unloading is employed in quasi-static contact problem and the concept of travelling finite elements is made use of in solving the steady rolling contact problem. The combined incremental and iterative procedure is adopted to solve these problems. The displacement function based finite element method is used to implement above algorithm. The results obtained are in good agreement with physical reasoning. The computational time and efforts have been greatly reduced by using skyline-storage for global stiffness matrix and sub-structuring methods.

CHAPTER I

INTRODUCTION

1.1 GENERAL INTRODUCTION

There are many instances in engineering structures, wherein the components are contacting one another and transfer external forces through the contact surfaces, such as shrunk-fit shaft and rotor, gear teeth in mesh, flanged connections of pressure vessels, dovetails of turbine blades, rolling wheel, etc. High stresses occur near contact zone leading to crack initiation and failure. This situation may occur in almost all types of mechanical assemblages. Therefore, it is important for the designer to understand the stress and deformation pattern in the vicinity of the contact surfaces. Accurate stress and strength analysis of such structures requires careful understanding of the frictional contact conditions.

In practical situations, the contact problems of different natures are encountered. The present investigation is aimed at elastic bodies in contact. These problems can broadly be classified into three categories:

A: Stationary Contact with no Friction

This occurs when two smooth bodies come into contact with each other along plane surface and transfer forces through it. No friction develops here. This is a linear problem because the

contact area remains unchanged during loading and also reversible as the system is conservative. This is the most simple problem and can be solved by direct application of principles of elasticity.

B. Varying Contact With no Friction

When two curved bodies with smooth surfaces come into contact, the area of contact is a function of load applied. When the contact area increases with the load, it is termed as advancing contact and receding contact vice versa. The change in contact area with loads renders the problem non-linear. However, it is still of reversible nature due to absence of non-conservative forces. Iterative procedures are adopted for solving such problems.

C. Varying Contact with Friction

When the nature of surfaces are frictional and the contact area varies with load, the problem comes under the category of varying contact and non-linear. The presence of friction makes the system irreversible and thus making it complex. This, in fact, is the most general case of contacting problems.

The present work is an attempt to solve these types of problems. Here, under the action of external loads, the domain of contact area and distribution of tractions are unknown over the contact region, thus, the contact problem is a non-linear problem with unknown boundary conditions. The existence of friction may lead to the formation of regions of slip and no-slip within the

contact surface. The relative magnitudes of tangential and normal tractions governs the status of contact surface. Also, the energy dissipated by the frictional forces makes the problem irreversible. Due to this the loading history also influences the final stress pattern.

Many analytical and numerical approaches have been attempted by many investigators in solving contact problems. The present work is an attempt towards using finite element method and principle of minimum dissipation of energy in solving two problems.

The first one, deals with a large plate with a circular hole having an inclusion subjected to slowly varying cyclic loading. This problem is of practical interest as all machines consists of many plates and are subjected to vibration. Another kind of commonly encountered contact problem is a rolling contact problem, where a body, having curved surfaces or boundary, rolls over other body which may be plane or curved. Such a phenomenon is found in many practical situations like tire-road contact, rail-wheel contact, ball and roller bearings, etc. In all these cases, during the rolling motion of one body over the other, the loads are transferred through contacting surfaces which keep changing continuously.

1.2 LITERATURE SURVEY

Contact problems have long been of considerable interest. Since, Hertz (1882) gave his well known classical solution of frictionless contact problem, further developments have taken place. The need for this in-depth study has come from practical

considerations particularly with respect to influence of interfacial friction. The following three basic approaches were adopted in solving these problems.

The earliest solutions have been obtained using integral equation methods. Existing exact solutions of contact stresses are the product of sophisticated mathematical analysis for idealised configurations. In many real situations, it is not possible to find suitable models for which closed form solutions are available. The exact solutions have been contributed by Mukhelishvili [1963] and Gladwell [1973], etc.

In later development, contact problems were considered as a special case of constrained optimization of either total potential or complementary potential energy. The minimization was formulated as a mathematical programming problems [Hung,198Ø].

In the third approach, contact conditions were imposed directly from kinematic considerations by imposing geometric compatibility of contacting surfaces during the incremental loading process. The main advantage of this method is that finite element procedures can be effectively used and the friction conditions can be imposed with ease. Finite element formulation can also be categorised in three types.

The flexibility method was developed by Francavilla and Zienkiewicz [1975] for frictionless elastic contact problems and then extended to frictional contact by Sachdeva and Ramakrishnan [1981]. Jing and Liao [199Ø] introduced the concept of relative displacements and contact double forces. Total loading and compatibility of displacements was used to determine the contact

forces. In second category, a stiffness matrix was used in the finite element formulation. Wilson and Parsons [1970] used differential displacements and a load incremental process to treat the frictionless contact problems. Chan and Tuba [1971] and Ohte [1973] studied the frictional contact problems for plane and axisymmetric elastic problems. Fredricksson [1976] proposed a constitutive model to account for friction at contact surface. Gaertner [1977] used an experimental friction law and a modified element to treat the connecting rod and Hertz problem. Okamoto and Nakajawa [1979] gave a finite element solution using incremental load theory. Torstenfelt [1983] and Rahman, Cook and Rowlands [1984] used iterative procedure for analysis of elastostatic contact problem with friction. Bathe and Choudhary [1985] solved for frictional contact under large deformation. Other researchers who contributed in the elastostatic field are Chandrasekaran, Haisler and Goforth [1987]. A variational approach, where the equilibrium and the boundary conditions were put into variational form, was adopted by Oden and Pires [1983]. They used a non-classical, non-local friction law and variational principle under which these laws hold.

Importance of rolling contact has also been considered by many authors. The different analytical and numerical solutions have been given by Poritsky [1950], Johnson [1958], Kalker [1979], etc. Kalker [1979] used the variation principle of Duvout and Lions for dry friction in solving three dimensional rolling contact problem with Hertzian normal contact. Liu and Paul [1989] developed a program to solve three dimensional rolling contact problems for arbitrary contact patches under arbitrary pressure distributions. The problem was considered with friction and non-Hertzian Pressure distribution. Padovan, Tovichakchaikul and Zeid [1981,1984] developed travelling finite elements based on the

use of a moving total/updated Lagrangian observer. They included large deformation kinematics and kinetics in the formulation.

The rolling contact problem was also described by a variational inequality (hyperbolic/elliptic) and solved numerically using incremental finite element method by Zochowski and Myslinki [1991]. They proposed a quasi-static approach and regularization of friction conditions. The problem was formulated as optimization problem and solved for normal contact tractions initially. The tangential contact stresses were calculated from regularised friction conditions.

The present work on the rolling contact, is an attempt to solve the problem by finite element method without assuming any distribution of tractions on the contact patch. The friction conditions are also not regularised and law of Coulomb's friction is followed. The concept of travelling finite elements is used to simulate the rolling effect.

Either in quasi-static or steady rolling problems, the friction contact problem has multiple solutions satisfying equilibrium conditions. As suggested by Kishore,N.N. [1979] and mentioned in the context of plasticity problems [Johnson and Mellor, 1973], it is proposed to use the concept of minimum dissipation of energy. That is, out of all the possible equilibrium configurations satisfying the new load conditions, the actual one leads to minimum dissipation of energy from the earlier state.

1.3 SCOPE OF PRESENT WORK

The author studied the steady rolling contact and quasi-static contact problems. In present study, finite element method coupled with principle of minimum dissipation of energy has been employed. In the rolling contact problem, the concept of travelling finite elements is used and a simple algorithm has been presented. No assumption regarding the distribution of tractions on the contact patch is made. In quasi-static contact problem, an incremental loading process has been adopted. The continuous loading and unloading, ranging from given maximum tension to that in compression, has been applied and corresponding response is obtained. Computer programs have been developed to solve these two types of contact problems and example problems are solved. In quasi-static contact problem, a large elastic plate with a hole having an oversized rigid inclusion is investigated. In rolling contact, a problem of steady rolling of a cylinder on a rigid plane surface, is solved.

The description of the problem formulation and solution techniques are detailed out in the following chapters. The theory of contact problem and the principle of minimum dissipation of energy are discussed in chapter II. Chapter III deals with the development of mathematical model and the solution scheme employed. The discussion on results is in chapter IV and chapter V summarizes conclusion of the present work and suggestions for future investigation.

CHAPTER II

THEORY OF CONTACT PROBLEMS AND MINIMUM DISSIPATION OF ENERGY APPROACH

2.1 BASIC THEORY OF CONTACT PROBLEM

Consider two generic bodies which are arbitrarily denoted as contactor and target (fig. 2.1a). The bodies are brought into contact by prescribed tractions and displacements applied on the surface S_t and S_u respectively. The target body can be either rigid or deformable. On coming into contact, the contact forces develop in the region of contact (fig. 2.1c), where neither the contact pressure nor the area of contact S_c is known a priori.

The basic conditions of contact along the contact surface is that no material overlap can occur (fig. 2.1b) and as a result contact forces are developed that act upon the target and contactor. The normal tractions can be only compressive in nature and the tangential tractions satisfy the law of frictional resistance. According to Coulomb's law of friction, the relative motion between two adjacent particles on the contactor and the target in contact can not occur, as long as $|\tau| \leq \mu |\sigma_n|$, where σ_n is the compressive traction, τ is the tangential traction and μ is a coefficient of friction. When $|\tau| > \mu|\sigma_n|$, the particles slide over each other and the motion continues as long as the tangential traction is developed to equal the limiting friction force $\mu\sigma_n$. Thus, the regions of no-slip and slip are identified and the following conditions are imposed as given below :

(i) stick or no-slip conditions

$$u_n^A = u_n^B$$

$$u_t^A = u_t^B$$
$$F_n^A = -F_n^B$$
$$F_t^A = -F_t^B \qquad (2.1)$$

u_n^A , u_n^B = Normal displacements of adjacent particles of body A and B, which are in contact.

u_t^A , u_t^B = Tangential displacements of adjacent particles of body A and B, which are in contact.

F_n, F_t are corresponding normal and tangential contact forces

(iv) slip conditions

$$u_n^A = u_n^B$$
$$u_t^A \neq u_t^B$$
$$F_n^A = -F_n^B$$
$$F_t^A = -F_t^B$$
$$F_t = \pm \mu |F_n| \qquad (2.2)$$

The direction of F_t and the tangential displacement are opposite in nature.

The same conditions of contact and friction apply to both quasi-static and rolling contact problems.

When a roller moves on a rigid plane surface without sliding, the contact develops between roller and ground. Within this contact area, some regions may be in slip and the other in no-slip condition. Generally, the micro-slip region is found in the leading edge and macro-slip occurs over trailing edge [Moore, 1975]. Since slip is an irreversible process, different loading histories would lead to different patterns of deformations. Three cases of rolling conditions are found in practical situations,

viz., free, driven and braked. In free rolling i.e. rolling under the action of a purely normal load, the extent of slip is small whereas when the contact surfaces transmit an externally applied tangential force or twisting couple, an appreciable amount of slip occurs.

Uniform rolling motion is a steady process in which the loads and the fields of stress, strain and deformation do not change with time with respect to an observer translating with the speed of roller. This is in contrast to quasi-static loading, where the stress-strain field and deformations changes with load. Therefore, the rolling contact problems are also termed as moving contact field or travelling load problems.

2.2 MINIMUM DISSIPATION OF ENERGY APPROACH

The elastic contact problem with finite friction is an irreversible problem, the solution to which depends upon the loading history. Here, not only the value of load but also the history of loading decides the direction of frictional resistance and hence the slip direction. In this problem, the loading and unloading are done gradually and the process is assumed to be quasi-static.

To explain the minimum dissipation approach, consider a system shown in the fig (2.2a). Let P is the load applied and F be the friction force developed. The force balance relation is

$$K X + F = P \qquad (2.3)$$

and also F is constrained as follows

$$F \leq \mu |N| \qquad (2.4)$$

The above relation and constraint has a feasible range for the displacement X for load level P1 and P2, shown in fig. (2.2b), is given by broken line. If the system were at a, at the load level P1, due to the load increment, it is proposed that it would go to the point b wherein, dissipated energy is minimum, in this case zero, and is feasible point. If it were at the point a', at the load level P1, even then it would move to the point b since it is that feasible point which has minimum dissipation, but unlike the previous case there is a finite amount of dissipation in this case.

The approach adopted by the present work is that after establishing the total contact area, the target is to decide about slip and no-slip regions. The principle of minimum dissipation of energy is employed to determine the extent of tangential displacement in the slip region.

The procedure of minimization of energy of dissipation and the search for the feasible state is formulated as a constrained minimization problem, with the dissipated energy expression, Φ_d, as the objective function together with a penalty due to constraints, e. The expression for Φ_d is given as :

$$\Phi_d = \sum_{k=1}^{m} \left| \left(\alpha_k^i - \alpha_k^{i-1}\right) * \left(\left(F_{t_k}\right)^{i-1} + \left(F_{t_k}\right)^i\right) / 2 \right| \qquad (2.5)$$

where the summation is over all m-contact node, α_k^i denote the tangential displacement of the node k on the contact surface at i^{th} load step and $F_{t_k}^i$, $F_{n_k}^i$ represent the tangential and normal nodal force at i^{th} load step.

The penalty term e ,takes into account the friction conditions given by :

$$e = \sum_{k=1}^{m} \left\{ \frac{(|F_{t_k}^i| - \mu|F_{n_k}^i|)^2}{\sqrt{\lambda}} + C * |(\alpha_k^i - \alpha_k^{i-1}) * (|F_{t_k}^i| - \mu |F_{n_k}^i|)| \right\} \qquad (2.6)$$

The first term in above expression is considered only for those nodes where $|F_t| \geq \mu|F_n|$. λ & C are penalty parameter and weighing factor, respectively.

To obtain the solution of constrained minimization problem, the objective function is modified by introducing penalty terms for the constraints. Now, the modified objective function is minimized, using a suitable unconstrained optimization technique.

Thus, the objective function to be minimized is :

$$\Psi = \Phi_d + e \qquad (2.7)$$

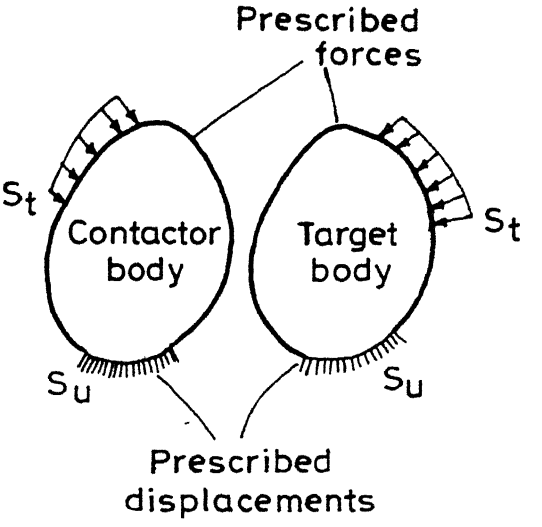
When Ψ is minimized, e usually becomes zero showing that all the nodes satisfy contact conditions and Φ_d also assumes a minimum of such possible states, then that state is characterized as a feasible state.

With the above notation, the sticking status of any node is represented as follows:

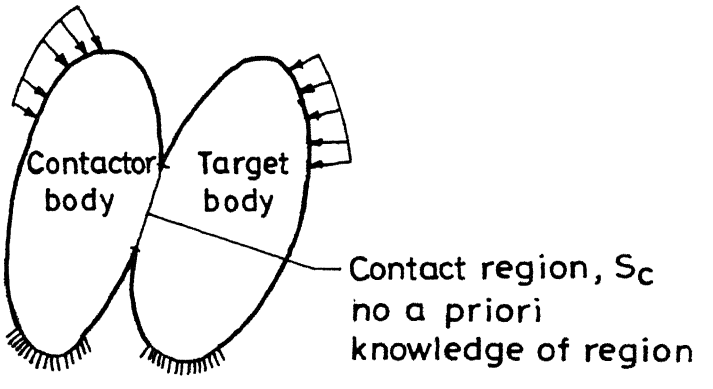
When $\alpha_k^i = \alpha_k^{i-1}$

$$e = \emptyset \text{ and } \Phi_d = \emptyset$$

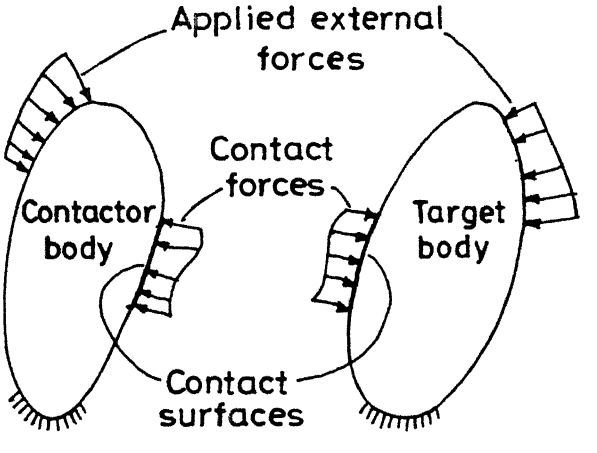
When e is not equal to zero then the set of unknowns α_k^i are found by minimizing Ψ. Thus, the extent of slip is determined.



(a) Condition prior to contact



(b) Condition at contact



(c) Forces acting on contactor and target body

Fig. 2.1 Schematic representation of a contact problem.

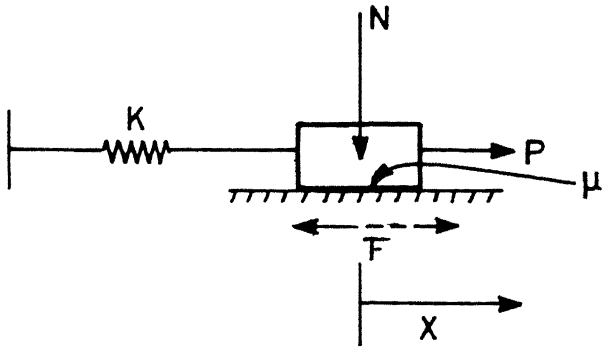


Fig.2.2(a) Example contact configuration.

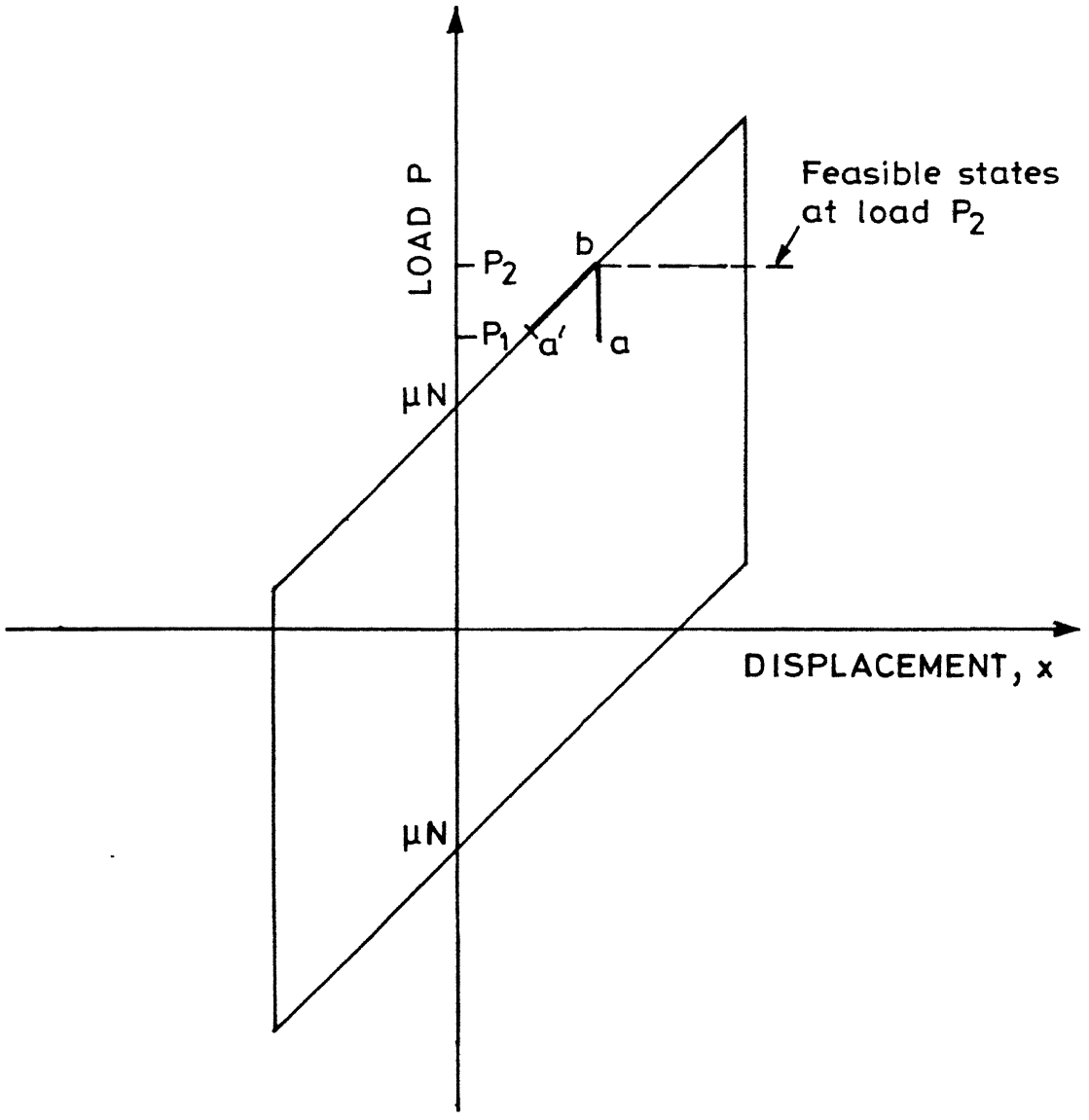


Fig.2.2(b) Feasible region.

CHAPTER III

FINITE ELEMENT METHOD AND SOLUTION ALGORITHM

The solution of the contact problem is determined in two stages. The first part is to determine the area of contact and the second part is to find the feasible state by principle of minimum dissipation of energy. The second part is the computer time intensive and hence sub-structuring methods are used to simplify the repeated calculations.

3.1 FINITE ELEMENT FORMULATION

To obtain a finite element solution, the following assumptions are made :

1. The materials are linear elastic.
2. The deformations are small.
3. Plane strain condition prevails.
4. The body forces are negligible.
5. The frictional force acting at the contact surface follows the Coulomb's friction law.
6. In case of rolling contact problem, the rolling speed is constant.
7. The rolling speed and mass are small enough, so that inertia forces can be neglected. Hence, the problem is quasi-static.

Consider a two-dimensional elastic contact problem with friction and separation. It is decided to use the stiffness formulation using displacement functions, as the contact algorithm can be implemented effectively and frictional condition can be enforced with ease.

The total potential energy functional in terms of stress functions is given as :

$$\Pi = \frac{1}{2}\int_V (\sigma_{ij} \epsilon_{ij}) \, dV - \int_V (X_i \, u_i) \, dV - \int_{S_t} (q_i \, u_i) \, dS \qquad (3.1)$$

where,

σ_{ij}, ϵ_{ij} stress and strain tensors respectively

$X_i . u_i$ body force components and corresponding displacements in volume domain V.

q_i , u_i surface tractions and corresponding displacements over the surface traction boundary S_t.

The first term in the above expression is strain energy and the last two are the work of body forces and surface tractions respectively.

To derive finite element formulation for the given functional, the domain is discretized into standard finite elements. Since the highest order of the derivatives present in the functional is one, minimum C° continuity is essential for the shape functions in the element selected. The simplest element satisfying this requirement is a constant strain triangular (CST) element i.e. a 3-noded triangular element. The derivation of

element stiffness matrix is described briefly in the following paragraph :

Assume displacement functions for 3-noded triangular element as :

$$u^x = a_1 + a_2 x + a_3 y$$
$$u^y = b_1 + b_2 x + b_3 y \qquad (3.2)$$

where u^x & u^y are displacement field in x & y directions, a's and b's are unknown coefficient.

The displacement functions can be represented in terms of nodal degrees of freedom as :

$$u^x = N_i\, u_i^x + N_j\, u_j^x + N_k\, u_k^x$$

$$u^y = N_i\, u_i^y + N_j\, u_j^y + N_k\, u_k^y \qquad (3.2)$$

where N's are interpolation function for CST elements, given as:

$$N_i = \frac{1}{2\Delta}\left[\bar{a}_i + \bar{b}_i\, x + \bar{c}_i y\right] \qquad (3.3)$$

where

$$2\Delta = \begin{vmatrix} 1 & x_i & y_i \\ 1 & x_j & y_j \\ 1 & x_k & y_k \end{vmatrix}$$

$$\bar{a}_i = x_j y_k - y_j x_k$$
$$\bar{b}_i = y_j - y_k$$
$$c_i = x_k - x_j$$

similarly, N_j and N_k can be determined.

The strain components for the element in terms of displacements are given as :

$$\{ \varepsilon \} = \begin{Bmatrix} \varepsilon_{xx} \\ \varepsilon_{yy} \\ \varepsilon_{xy} \end{Bmatrix} = \begin{Bmatrix} \partial u^x / \partial x \\ \partial u^y / \partial y \\ \partial u^x / \partial y + \partial u^y / \partial x \end{Bmatrix}$$

$$\{ \varepsilon \} = [B] \{ u \} \qquad (3.4)$$

where,

$$[B] = \frac{1}{2\Delta} \begin{bmatrix} \bar{b}_i & \emptyset & \bar{b}_j & \emptyset & \bar{b}_k & \emptyset \\ \emptyset & \bar{c}_i & \emptyset & \bar{c}_j & \emptyset & \bar{c}_k \\ \bar{c}_i & \bar{b}_i & \bar{c}_j & \bar{b}_j & \bar{c}_k & \bar{b}_k \end{bmatrix}$$

$$\{u\} = \begin{Bmatrix} u_i^x \\ u_i^y \\ u_j^x \\ u_j^y \\ u_k^y \\ u_k^y \end{Bmatrix}$$

The stress-strain components are related by the material property vector [D] as:

$$\{\sigma\} = [D]\ \{\epsilon\} \qquad (3.5)$$

For Plane Stress,

$$[D] = \frac{E}{1-\nu^2}\begin{bmatrix} 1 & \nu & \emptyset \\ \nu & 1 & \emptyset \\ \emptyset & \emptyset & \frac{1-\nu}{2} \end{bmatrix} \qquad (3.6)$$

For Plane Strain,

$$[D] = \frac{E}{(1+\nu)(1-2\nu)}\begin{bmatrix} 1-\nu & \nu & \emptyset \\ \nu & 1-\nu & \emptyset \\ \emptyset & \emptyset & \frac{1-2\nu}{2} \end{bmatrix} \qquad (3.7)$$

where E and ν are the modulus of elasticity and Poisson's ratio.

The given functional, neglecting body forces :

$$\pi = \frac{1}{2}\int_V (\sigma_{ij}\,\epsilon_{ij})\,dV - \int_{S_t} (q_i\,u_i)\,dS \qquad (3.8)$$

Taking the matrix form and by substitution -

$$\pi = \frac{1}{2}\int_V \{\epsilon\}^T[D]\ \{\epsilon\}\,dV - \int_{S_t} (q_i\,u_i)\,dS$$

$$= \frac{1}{2} \int_V \{u\}^T [B]^T [D]\ [B]\ \{u\}\ dV - \{u\}^T \{F\}$$

$$= \frac{1}{2} \int_V \{u\}^T [K]\ \{u\} - \{u\}^T\ \{F\}$$

where $[K]^e = \int_V [B]^T\ [D]\ [B]\ dV$

= Stiffness matrix of a triangular element.

Minimizing Π with respect to nodal displacements and it results into set of equations

$$[K]\ \{u\} = \{F\} \qquad (3.9)$$

where

[K] = Global stiffness matrix = $\sum [\ K\]^e$

{u} = Nodal displacement vector

{F} = Nodal force vector = $\sum \{\ F\ \}^e$

The system of equations for two bodies in contact can be combinedly written as

$$\begin{bmatrix} K^A & \vdots & \emptyset \\ - - & \vdots & - - \\ \emptyset & \vdots & K^B \end{bmatrix} \begin{Bmatrix} U^A \\ - - \\ U^B \end{Bmatrix} = \begin{Bmatrix} F^A \\ - \\ F^B \end{Bmatrix} \qquad (3.10)$$

where,

K^A , K^B stiffness matrix of two bodies A & B respectively.

U^A , U^B displacement degrees of freedom of bodies A & B respectively.

F^A, F^B the force degrees of freedom of bodies A and B respectively

For any problem, the accuracy of the solution also depends upon the mesh size but at the cost of computational efforts. A good compromise is to consider a fine mesh in the region of high stresses i.e. in the vicinity of contact surface and coarser mesh away from this region.

In the present investigation, for simplicity, it is assumed that one of the two contacting body is rigid, whereas the other one is deformable which needs to be discretized only. Symmetry has been made use of wherever present. At the contact surface, local coordinate system, having tangential and normal directions, are considered. For solving above equations the contact conditions have to be enforced and they are described in the following section.

3.2 CONTACT CONDITIONS

As stated above, one of the two bodies in contact is taken as rigid one, the set of equations corresponding to that body need not be considered. Hence, eq. (3.1Ø) simplifies to

$$[K] \{ U \} = \{ F \} \qquad (3.11)$$

The solution of the above set of equations is subjected to boundary conditions. There are two kinds of boundary conditions in contact problems, viz. prescribed and contact. The prescribed boundary conditions are in terms of externally applied tractions and displacements. The contact boundary conditions are not known a priori and are determined in two phases.

Phase I : Determination of contact area

Initially, a set of possible nodes is considered in contact and the response is obtained at given load level. If at a node, the normal contact force turns out to be tensile then, that node is set free. Whereas, if the displacement of any free node, in normal direction of contact surface, appears to penetrate geometrically or touches the rigid surface, it is included in the contact region.

Thus, the following conditions are imposed when the node changes their state :

(i) Change from Contact to Separation

In the separated condition, the node is treated as a free node and their nodal force components are equated to zero.

$$F_n = \emptyset$$
$$F_t = \emptyset$$

F_n, F_t are normal and tangential contact forces respectively.

(ii) Change from Separation to Contact

The displacement conditions in normal and tangential directions are modified so that the given node becomes a contact node as :

$$u_n = \delta$$
$$u_t = \emptyset$$

where,

u_n is a normal nodal displacement

δ is a clearance between the rigid surface and the corresponding node in normal direction before application of the given load

u_t is the tangential nodal displacement which is negligibly small.

Using the above conditions at the corresponding nodes, the response in terms of reaction contact nodal forces at the contact zone and displacements of free nodes is obtained. Again, the conditions of contact are checked and the above procedure is repeated, till the contact conditions no more changes at the given load in successive iterations. Now, all the nodes in contact will have compressive normal force.

Phase II : Determination of Slip and No-slip Zones in the Contact Region

Having determined the contact area at a load level, the next phase is to check the friction condition to establish the regions of slip and no-slip as given below:

Let μ be the coefficient of friction and F_n and F_t be the normal and tangential nodal contact forces.

(i) when $|F_t| \leq \mu |F_n|$, both the contact surfaces adhere to each other i.e. there is no relative tangential displacement between the node and the rigid-surface.

For this case, the following conditions are imposed as:

$$u_n = \delta$$
$$u_t = \emptyset$$

(ii) When $|F_t| > \mu|F_n|$, the node tends to slip over the rigid surface i.e. the node will have relative tangential displacement The nodes are allowed to slip by extent such that $|F_t| = \mu |F_n|$. The direction of F_t is chosen such that it opposes the tangential movement of the node with respect to rigid surface. The new solution satisfying all conditions is determined by the approach discussed in sec. 2.2. The two types of problems are studied in the present work.

3.3 APPLICATION TO QUASI-STATIC LOADING

In this, a plate with a hole with an oversized rigid inclusion is studied. The contact between the plate and inclusion is due to mechanical friction only. The plate is subjected to farfield uniform loading. The loading and unloading processes are done gradually and after each load increment, the solution is updated. In such problems, the load increments are chosen in such a manner that at a time either one node comes into contact or just one node separates, and the changed contact conditions at the node are assumed to become operative for subsequent load increments. The expressions for interpolating the incremental load is discussed below as :

First, solve for a nodal displacement increment $\{\Delta U_n\}$ and a contact force increment vector $\{\Delta F_n\}$ using the contact conditions of previous step and a test load $\{\Delta P\}$. $\{U_n\}$ and $\{F_n\}$ are solution at load P_n.

The new load P_{n+1} is found as -

$$\{P_{n+1}\} = \{P_n\} + \alpha_n\{\Delta P\} \qquad (3.12)$$

where α_n is a load incremental ratio. The value of α_n is smallest of α_n^* (It is a value of load incremental ratio at different nodes) calculated for the nodes violating their existing contact conditions. The following two cases are considered :-

1. From Separation to Contact Condition

$$l_{N,n+1} = l_{N,n} + \alpha_n^* \cdot \Delta l_{N,n} = \emptyset \qquad (3.13)$$

So,

$$\alpha_n^* = - l_{N,n} / \Delta l_{N,n} \qquad (3.14)$$

l_N and Δl_N are the clearance between two bodies in normal direction before the application of incremental load and change in clearance over the incremental step respectively.

2. From Contact to Separation Condition

$$F_{N,n+1} = F_{N,n} + \alpha_n^* (\Delta F_{N,n}) = \emptyset \qquad (3.15)$$

So,

$$\alpha_n^* = - F_{N,n} / \Delta F_{N,n} \qquad (3.16)$$

F_N is normal contact force component before application of incremental load.

ΔF_N is incremental normal contact force component

The same criterion of contact and friction apply as discussed in the sec. 3.2. In this problem, because of the interpolation of load increments, a new node is included in the contact zone when it has just touched the rigid surface, hence the normal clearance δ is always zero. When the condition of slip is encountered, the extent of slip is determined by the approach discussed in section 2.2. The dissipation of energy, ϕ_d (Eq.2.3) and penalty term, e (Eq.2.4) are reproduced below :

$$\Phi_d = \sum_{k=1}^{m} | \ (\alpha_k^{i-1} - \alpha_k^i) * ((F_{t_k})^{i-1} + (F_{t_k})^i) * / \ 2 \ | \qquad (3.17)$$

where Φ_d represents the sum of the dissipation of energy at all m-contact nodes.

The penalty term e , takes into account the friction conditions as given by :

$$e = \sum_{k=1}^{m} \left\{ \frac{(|F_{t_k}| - \mu|F_{n_k}|)^2}{\sqrt{\lambda}} + C * |(\alpha_k^{i-1} - \alpha_k^i) * (|F_t| - \mu|F_n|)| \right\} \qquad (3.18)$$

Thus, the objective function is :

$$\Psi = \Phi_d + e \qquad (3.19)$$

The Objective function Ψ, which includes the penalty, e and the dissipation of energy, Φ_d, is minimized by a suitable unconstrained minimization technique. Hookes and Jeeves pattern search method [Rao S.S., 1990 and Kuester-Mize, 1973], which is a

unimodal, sequential search type, is adopted in determining the tangential displacements, represented as the geometric variables α_k, such that the dissipation is minimum and all other constraints are satisfied. For the kind of objective function, formed in this problem, the Hooke and Jeeves pattern search method is found to be quite effective. This method can handle no. of variables simultaneously and convergence is guaranteed.

In this method probing function evaluations are made in all the directions and as shown in fig. 3.2, for two variable search. The variables are perturbed sequentially and pattern direction, S, is found. The variables are given one step in the pattern direction before the search for a new direction is made. If search fails to yield a decrease in the value of the objective function, the pattern step is retraced and the search for pattern direction is made with half the step size. This is carried on till the convergence is reached or the step size becomes less than a specified value.

3.4 APPLICATION TO ROLLING CONTACT

As discussed in sec. 2.1, in rolling contact phenomenon, new nodes enter the contact zone and some leave it continuously, as rolling proceeds. It may be noted that the number of nodes in contact at any instant during steady rolling, remains constant. New nodes enter the contact zone at the leading edge and as the body keeps rolling, the locations of the nodes shift rearwards. Before the nodes leave contact, they have traversed through the complete contact zone. This is depicted in fig. 3.3, where nodes occupy different locations at time t_1, t_2 and t_3. During the rearward journey, the nodes undergo continuously varying stress-strain field along the contact length. Also, in rolling

motion, the spatial co-ordinates of every point of body changes, making modelling of such a problem difficult task. To overcome this, in present study, the concept of travelling finite elements is used. It may be noted that in case of steady rolling the stress-strain field and deformations over contact area remain same with respect to system translating with speed of centre of roller.

The method is based upon the fact that every material point or node on the periphery of rolling body passes through the entire contact field during its period of contact. For example, as shown in fig. 3.3, while the body rolls from instant t_1 to t_2, node 1 separates and node 5 enters the contact field. The external traction field is same for both situations. Under the steady state conditions, node 2 at instant t_2, would have the same conditions of contact, as node 1 was having at the instant t_1. Similarly, node 3 replaces node 2 and so on. Thus, the steady contact field is occupied by a newly formed set of nodes as the body rolls.

In the present method, the above discussed feature of rolling contact is exploited. So, instead of actually rolling the body, the contact field conditions are shifted rearward over the contact nodal points. The contact zone is considered to be formed by the same set of nodal points for all iterations.

The methodology of implementing the above algorithm is discussed herewith. To start with, the transient response at instant t is assumed to be known and rolling is assumed to take place in steps of one-degree which coincides with the distance between nodes in contact.

Let the contact be at n nodes as shown in fig.3.4 and the direction of rolling as shown. From the previous discussions the displacement boundary condition in tangential direction at the i^{th} node at instant t+Δt is taken as :

$$u_i \text{ , at time } t+\Delta t = u_{i+1}, \text{ at time } t$$

subscript i represents a node in contact zone.

The normal displacement boundary conditions which are the results of kinematic constraints are taken constant for all iterations. Using these displacement boundary conditions, the response at instant t+Δt is obtained in terms of contact nodal forces. Now, the friction condition is checked at all the contact nodes to decide the contact status. Those nodes for which the ratio of tangential to normal traction exceeds the coefficient of friction, are allowed to slip. The extent of slip is determined using the minimum dissipation of energy approach. The direction of F_t opposes the slip at the node and the slip is equal to the change in displacement of that node while body has rolled from instant t to t+Δt. The equivalent of the slip in present method can be taken as $(u_i^{t+\Delta t} - u_{i+1}^{t})$. The subsequent iterations are carried out in similar manner till the response converges to a steady state one.

The solution of rolling contact is obtained in two stages. In first stage, for the given external traction conditions, the static equilibrium solution is obtained. Then, in the second stage, the rolling criterion, as discussed above, is used to get the final steady state solution. The initial solution at any stage is obtained by taking sticking conditions at all nodes in contact. To decide about the region of slip, the nodes are

checked for the relative magnitude of tangential and normal traction. At the nodes, satisfying the condition of slip, the extent of slip is determined using the principle of minimum dissipation of energy. The nodes are allowed to slip sequentially and their order of sequence is procedurally determined such that the resultant configuration has followed the path of minimum dissipation of energy. The friction condition is put at the nodes which are set to slip and the tangential displacements are obtained.

3.5 IMPLEMENTATION DETAILS

In addition to putting the boundary conditions the solution of any problem requires the considerations of many other factors in order to make the program efficient and computationally economical.

The global stiffness matrix [K], here, is symmetric and banded. To exploit these characteristics, it is stored in skyline form. Routines described in reference [Fellipa, 1974] are used for solution of matrices of such data structures.

In this problem, the contact conditions i.e., a node coming into contact or a node separating or change in friction status of slipping or sticking when imposed, will change the stiffness matrix. Hence, the stiffness matrix gets modified in every iteration. However, the changes are only in the equations corresponding to the possible contact nodes. Also, the known displacements of the nodes can be eliminated from the solution system. Hence, a multi level sub-structuring scheme is made use so that a smaller matrix is handled in the iterative procedure.

The sub-structuring scheme is necessary not only to save the computational time but also because the contact displacement and force relations, if imposed, render the stiffness matrix unsymmetrical, and hence requiring full storage. Sub-structuring enables smaller matrix, consisting of equations corresponding to the contact nodes only, to be stored and operated upon in every iteration. The main steps of sub-structuring are given in the Appendix A.

To obtain the response for an incremental step, the changed contact conditions are imposed iteratively, till the solution becomes consistent. The contact conditions, as mentioned in section 3.2, are imposed on the condensed stiffness matrix, which economizes the computer efforts. The exact methodology of imposition of these conditions is discussed in APPENDIX B.

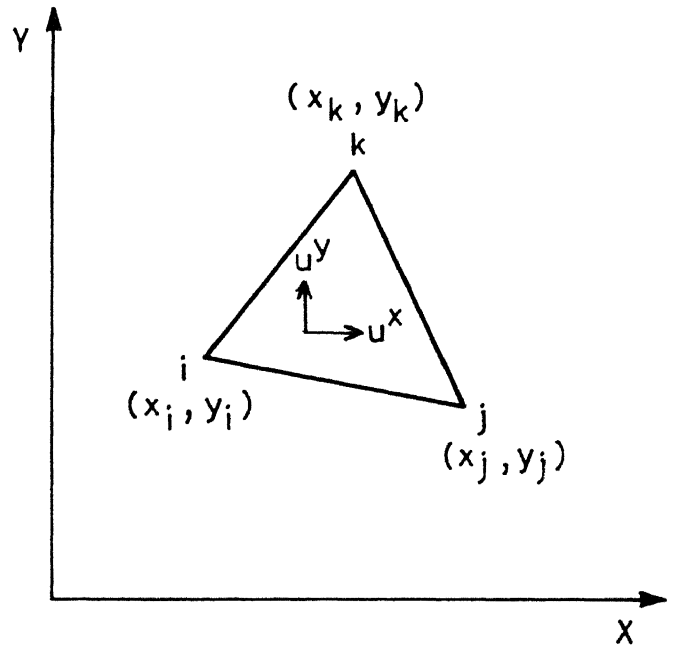


Fig.3.1 A representative CST element.

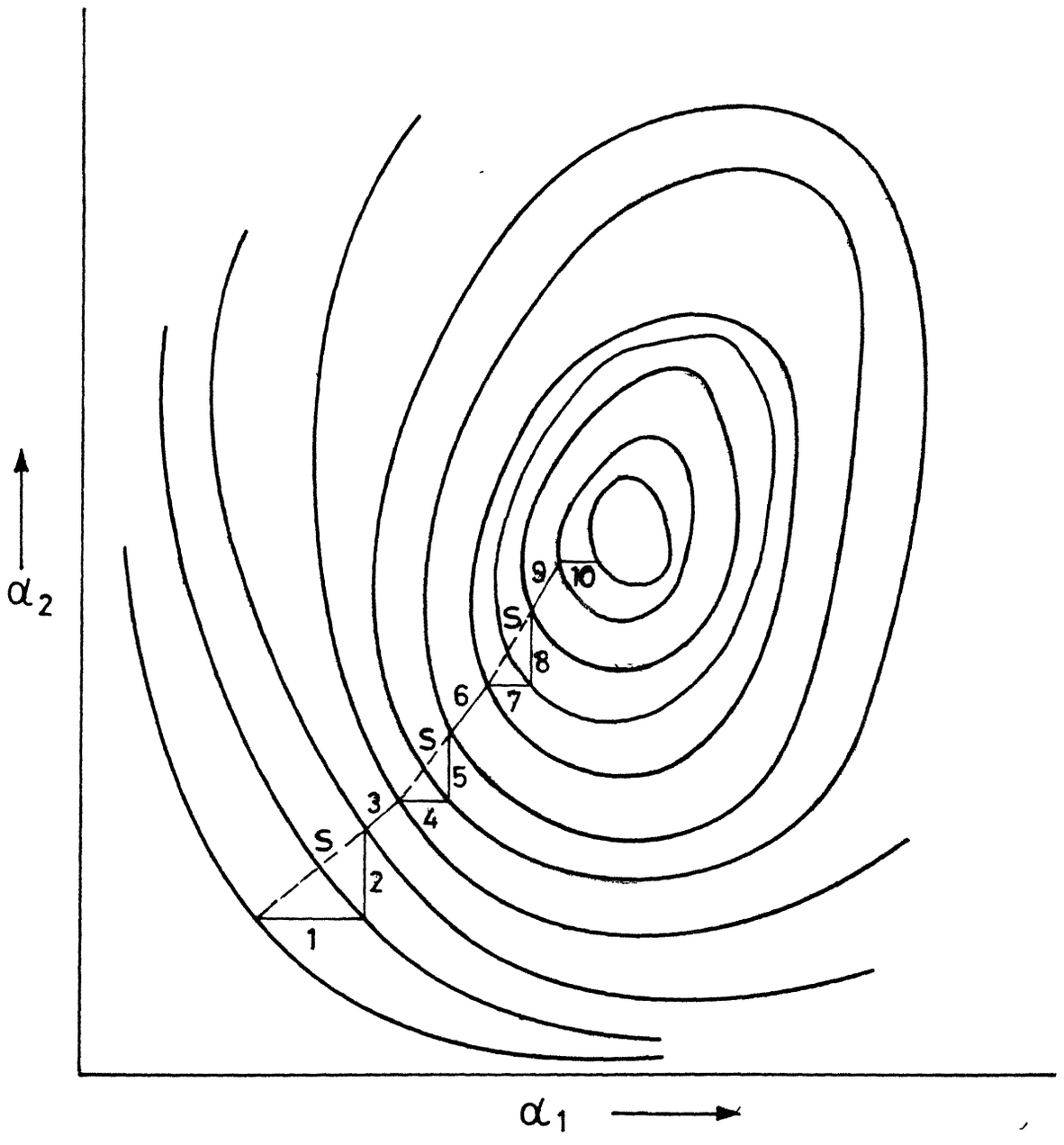


Fig. 3.2 Minimisation search algorithm.

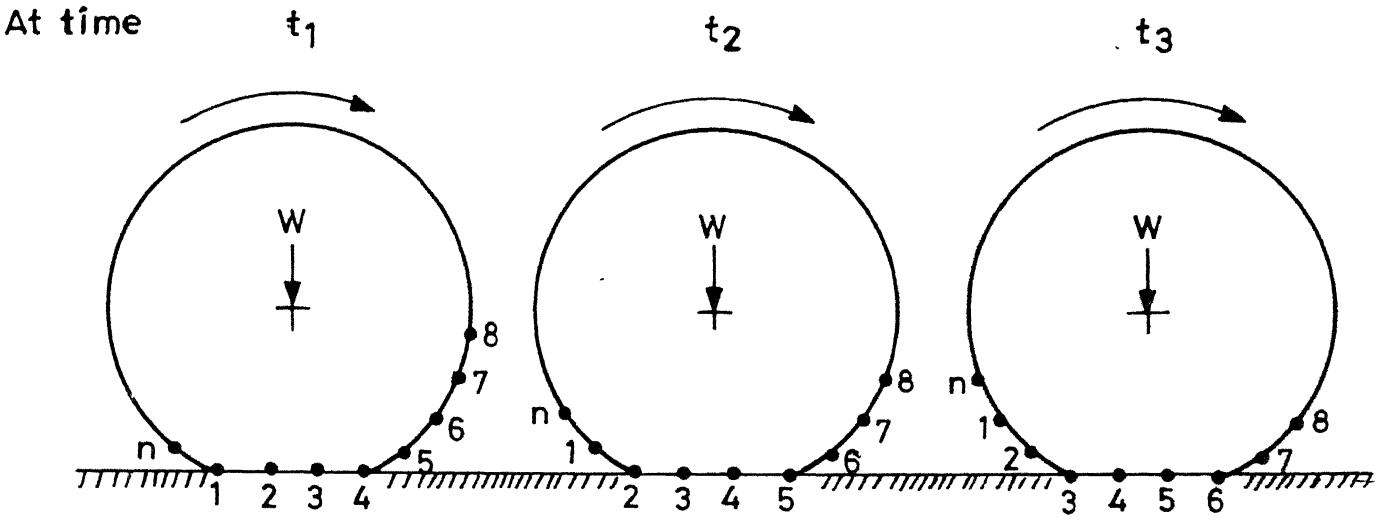


Fig. 3.3 Different instances of rolling motion.

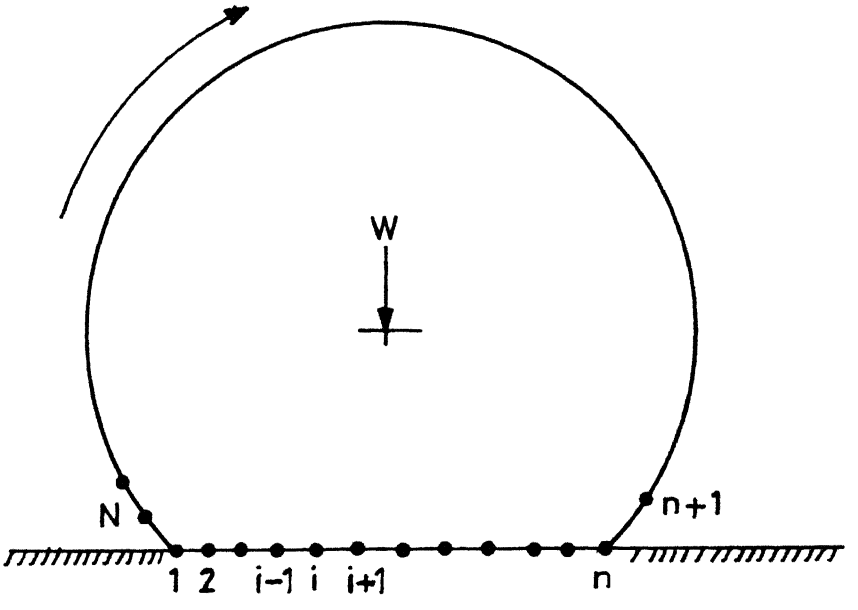


Fig. 3.4 Typical representation of 'n' nodes being in contact.

CHAPTER IV

RESULTS AND DISCUSSION

As discussed in earlier chapters two problems are analysed to investigate the effectiveness of the proposed algorithm. The first one is a plate with a hole having an oversized rigid inclusion, subjected to quasi-static loading and unloading. In second problem, the steady rolling of a cylinder on a rigid surface is studied. The validity of the results is also discussed.

4.1. A Plate with a hole and inclusion

As explained earlier the plate is assumed to be thick (Plane Strain condition) with a circular hole. An oversized rigid circular inclusion is embedded in the hole. The plate is subjected to a uniform farfield external loading (fig. 4.1a). The loading is assumed to be slowly varying, cyclic in nature, satisfying the quasi-static assumption. A finite plate with a/r = 6 is taken to simulate a large plate. Because of symmetry it is enough to analyse one-quarter of the plate and the geometry is shown in fig. 4.1b along with finite element mesh. As shown in the above figure, there is a fine mesh near the hole boundary and coarser mesh away. The actual mesh used for analysis is still finer with 360 elements and 207 nodes.

In what follows the oversizedness of the rigid inclusion is expressed in terms of an equivalent initial precompression stress, T_{pre}, as

$$\bar{T}_{pre} = - \frac{\delta}{r} \frac{E}{(1 + \nu)} \qquad (4.1)$$

δ amount of precompression
r radius of hole
E modulus of elasticity
ν Poisson's ratio

The material properties and geometry of the plate are taken as

$E = 30.0E06$ Pa
$\nu = 0.25$
$r = 1$ cm
$a = 6$ cm
$\delta = 1.5E-04$ cm

The external loading in terms of displacements is applied. It is assumed that there are no locked displacements initially and the tensile load is applied gradually.

4.1.1 Comparison of the Solution Methods : with and without the energy dissipation term

The quasi-static problem is analysed by two methods to evaluate the effectiveness of the dissipation of energy term. Thus, while determining the slip, no-slip and separation zones by minimizing the objective function the solutions are obtained by two methods :

I objective function, Ψ consists the error due to constraints, e only (This method is referred as 'without dissipation of energy')

II objective function consists the error due to constraints, e as well as the energy dissipation, Ψ_d. (This method is referred as 'with dissipation of energy')

Fig. 4.2 presents the contact zones as function of load T (non dimensionalized as T/T_{pre}) while the load is applied in tension for a coefficient of friction, μ, of 0.1 by the method I

('without dissipation energy') and fig. 4.3 presents the results of the same problem by the method II ('with dissipation energy term'). From the figures it is clear that with the increase in load, slip zone appears first and expands. Later the nodes near 90° begin to separate and spread inward. It can be observed that there is no difference in the results by the two methods, though, first method requires interpolation of load for any node going from no-slip to slip state. Figs. 4.4 and 4.5 presents similar results for a coefficient of friction, μ, of 0.4. Qualitatively, the behaviour is same as those for μ=0.1 except that no-slip zones are bigger. Because of the coarseness of the mesh the data are not available very much near to 0° and 90°, the present curves are extrapolated (shown by dashed line) for the sake of completeness and understanding.

Figs. 4.6 and 4.7 present the variation of contact zones with load when the load is decreased from the maximum tensile load (referred to as 'unloading tension'). Results have been obtained for a coefficient of friction, μ=0.1 by the method I and the method II respectively. During this unloading process, the nodes tend to slip in the direction opposite to that while loading and is opposed by frictional forces. As unloading proceeds, for a fraction of load step the slip zone becomes no-slip. The nodes in no-slip zone go to slip gradually and the size of separation zone decreases and it changes into slip zone. It can be seen that the same behaviour is obtained by both the methods. Whereas at the higher coefficient of friction, μ=0.4 (figs. 4.8 and 4.9), the methods differ. It can be observed that in case of method I (fig. 4.8) when any node enters the contact zone from separation, it slips. Later on, the nodes near 90° go to no-slip zone. On the other hand, method II (fig. 4.9) shows that the nodes near 90° directly go to no-slip zone. After investigating the two methods, it was found that in case of method I, the nodes near 90° simply oscillates between slip and no-slip conditions. It requires a finer mesh to get correct solution with method I, whereas method II can tackle such situations effectively even with present mesh.

After completely unloading, it is loaded in compression to the same maximum value as that in tension. The figs. 4.6 to 4.9 show the bahaviour during that process and found to be comparable for both methods.

During unloading from maximum compression, in case of method I ('without dissipation of energy'), fig. 4.1Ø (for μ = Ø.1) shows that there is complete no-slip zone at the interface initially and slip zone appears as unloading continues. Whereas, by the method II ('with dissipation of energy') some of the nodes slip in the same direction as that while loading. As the unloading proceeds some of those nodes stick for some time and then start slipping in the reverse direction. This complex behaviour is not obtained by the method I procedure. Praobably, it may be possible to obtain this complex bahaviour by the method I also, if a very fine mesh and small load steps are used. Thus, it can be inferred that minimization of dissipation of energy during loading steps aids in the determination of the complex contact conditions more accurately with ease.

4.1.2 Stress Variation at the Interface

The distribution of normal and tangential stresses at the interface is presented in figs. 4.14 to 4.17, with stresses being non-dimensionalised with respect to farfield applied stress, for different coefficients of friction.

Fig. 4.14 presents the distribution of normal stress at the maximum tensile load. As expected the stress is maximum near $Ø^{o}$. It can also be observed that, σ_n maximum, decreases with increase in coefficient of friction. There is a slight deviation near the plane of symmetry, which may be due to angular contact area [Gaertner, 1977] and use of lower order element in the region of high stress gradient. There exists a separation zone also at this load, shown as zero contact stresses.

The distribution of tangential stress at maximum tensile load is shown in fig. 4.15. The curves are extrapolated, shown by dashed lines, to represent values of stress near to $\theta=\emptyset^{\circ}$ and outermost edge of contact. The distribution is consistent with friction conditions present at interface.

Figs. 4.16 and 4.17 present normal and tangential stress distribution at the maximum compressive load. It may be seen that as the effect of friction increases the σ_n becomes flatter and the σ_n maximum has a higher value for lower coefficients of friction whereas σ_t maximum is lower for lower coefficients of friction. The normal stress distribution has depression near both the plane of symmetry. The effect of friction upon it is as expected.

4.2 A Cylinder rolling on a Rigid plane surface

As mentioned earlier in the case of a cylinder rolling on a horizontal ground, the rolling is assumed to take place at a uniform speed and speed is very low. As the horizontal ground is assumed to be rigid and the cylinder is elastic, for the finite element analysis it is enough to discrete the cylinder. Details of the geometry and the typical mesh used is shown in fig. (4.18 a and b). Mesh is finer near the contact zone with the ground. Actual mesh used is still finer with 1548 elements and 847 nodes. The nodes within fine mesh are positioned at one degree of angle apart on the periphery. The flat bed is modelled as an infinite dimensional bed but all the displacements of the bed are taken zero to depict rigidity. The W and P are normal and driving tangential load on the cylinder and F_R is considered for losses like windage, etc and in the present study it is taken constant as $F_R/W = \emptyset.\emptyset2$.

As explained in sect. 3.4, the initial configuration is taken to be the static solution and rolling is effected in steps of one

degree so that the nodal contact conditions are translated to the left by one node at a time. In each iteration nodal conditions are modified to satisfy the contact conditions in a sequence so as to minimize the dissipation of energy. This procedure is continued until steady contact conditions are obtained arriving at steady rolling configuration.

The solution obtained, satisfies all the physical laws applicable and all the characteristics of the rolling contact. Figures 4.19 and 4.20 show the distribution of normal and tangential forces at the contact nodes for different coefficients of friction, for a P/W = 0.04. The nodal force components are non-dimensionalised. The location of centre of the cylinder is represented by a single dash centre line in all the figures. As discussed in various literatures [Moore, 1975], the slip regions exist over the leading and trailing edge only. The intermediate portion of the contact is of no-slip nature. The extent of slip over the leading edge(L.E.) is very small($\sim 1^{o}$) and of significant magnitude over the trailing edge(T.E.) ($\sim 4\text{-}5^{o}$), thus agreeing with the concept of micro and macro slip over leading and trailing edge.

The overall contact area and normal stress distribution are essentially same for different coefficients of friction (fig. 4.19). As can be seen in the fig. 4.20, the tangential stress varies linearly near the middle portion of the contact and attains maximum values near the edge and assumes zero values at the ends of contact zone. The overall maximum occurs in the trailing edge and higher for higher coefficients of friction. Fig 4.21 shows the size of various contact zones at different coefficients of friction. It is clear from this figure that there occurs slip zones at the either edge (As already mentioned) and they decrease significantly as the coefficient of friction increases. Figure 4.22 and 4.23 presents the variation of normal and tangential nodal force components in the contact zones for various P/W values. This brings out the fact, as expected, that as the P/W increases the contact area shifts towards the leading edge. The

normal stress distribution more or less remains same whereas the tangential increases with P/W.

Effect of changing P and W keeping P/W constant on the contact stresses can be seen in fig. 4.24 and 4.25. It can be observed that the overall contact length increases with P, but the variation is of the same nature.

Energy dissipation per degree rotation is evaluated for different cases and presented in fig. 4.26 & 4.27. In fig. 4.26 the variation of energy dissipation with P/W for higher coefficients of friction is shown. It may be noted that the energy dissipation increases with P/W. Fig. 4.27 presents variation of energy dissipation with coefficient of friction for various P/W values. The dissipation of energy is low at a very low coefficient of friction and increases with the μ, attains a maximum value and decreases with further increase of μ. Thus, it clearly shows that for lower dissipation of energy, it is required to have a very low or high value of coefficient of friction.

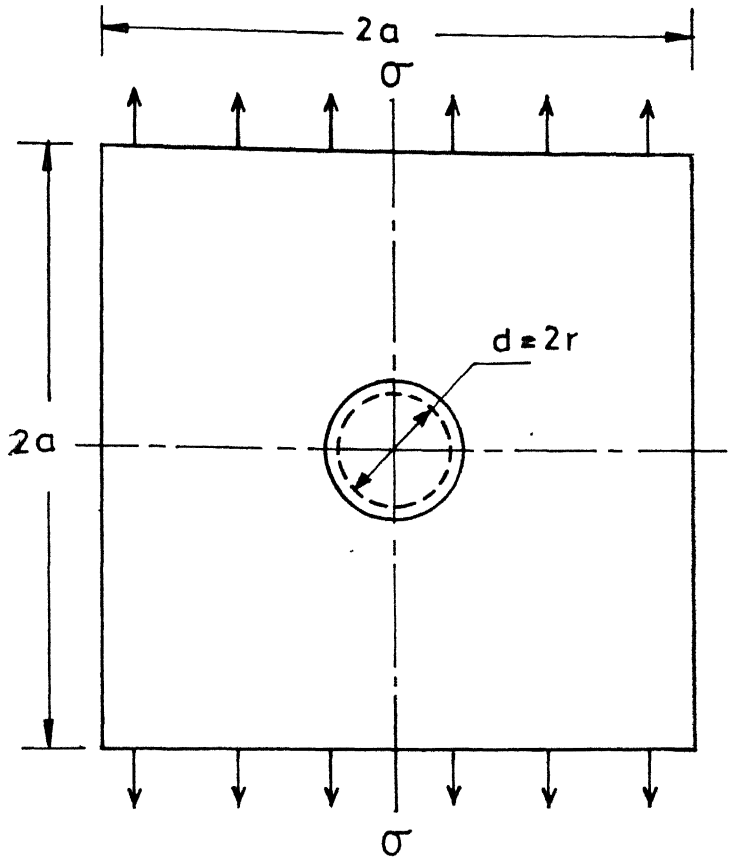


Fig. 4.1 (a) A plate with a oversized rigid inclusion

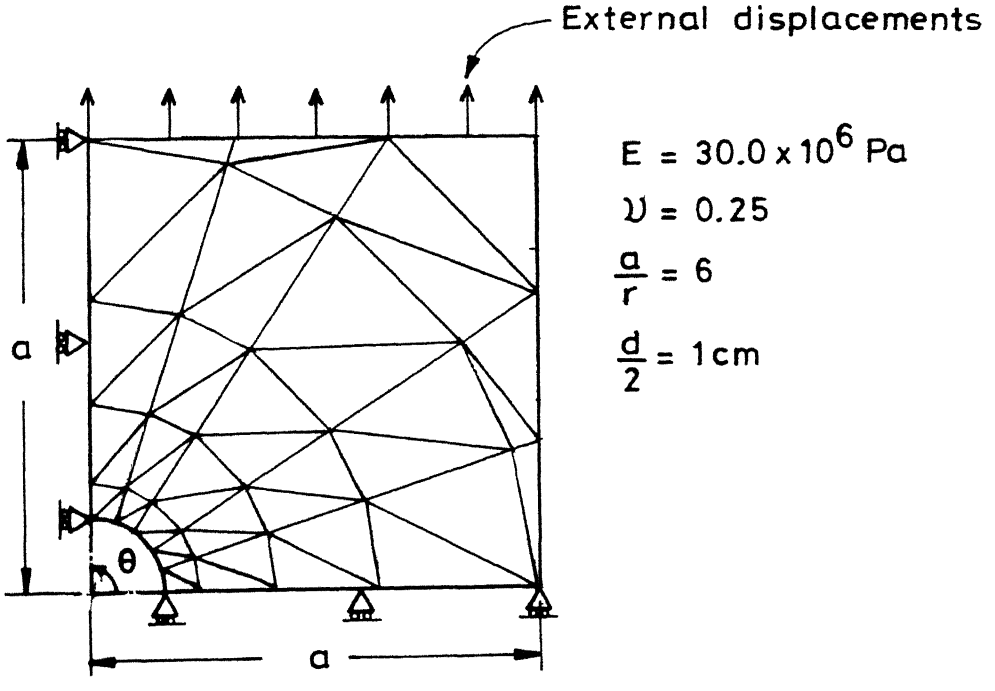


Fig. 4.1 (b) Representative mesh and prescribed boundary conditions.

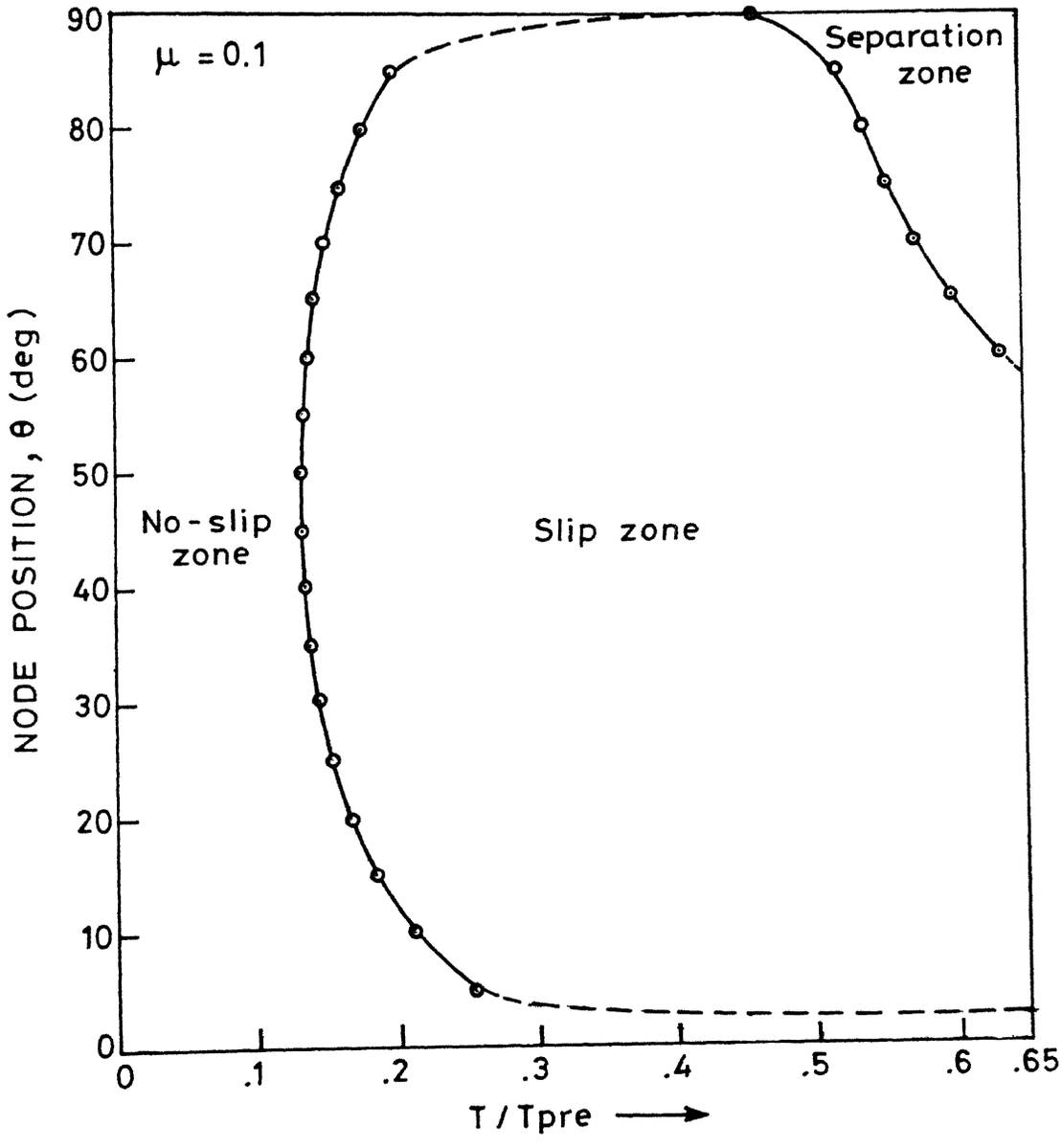


Fig.4.2 Interface zones while loading in tension from undeformed state (without minimizing energy of dissipation)

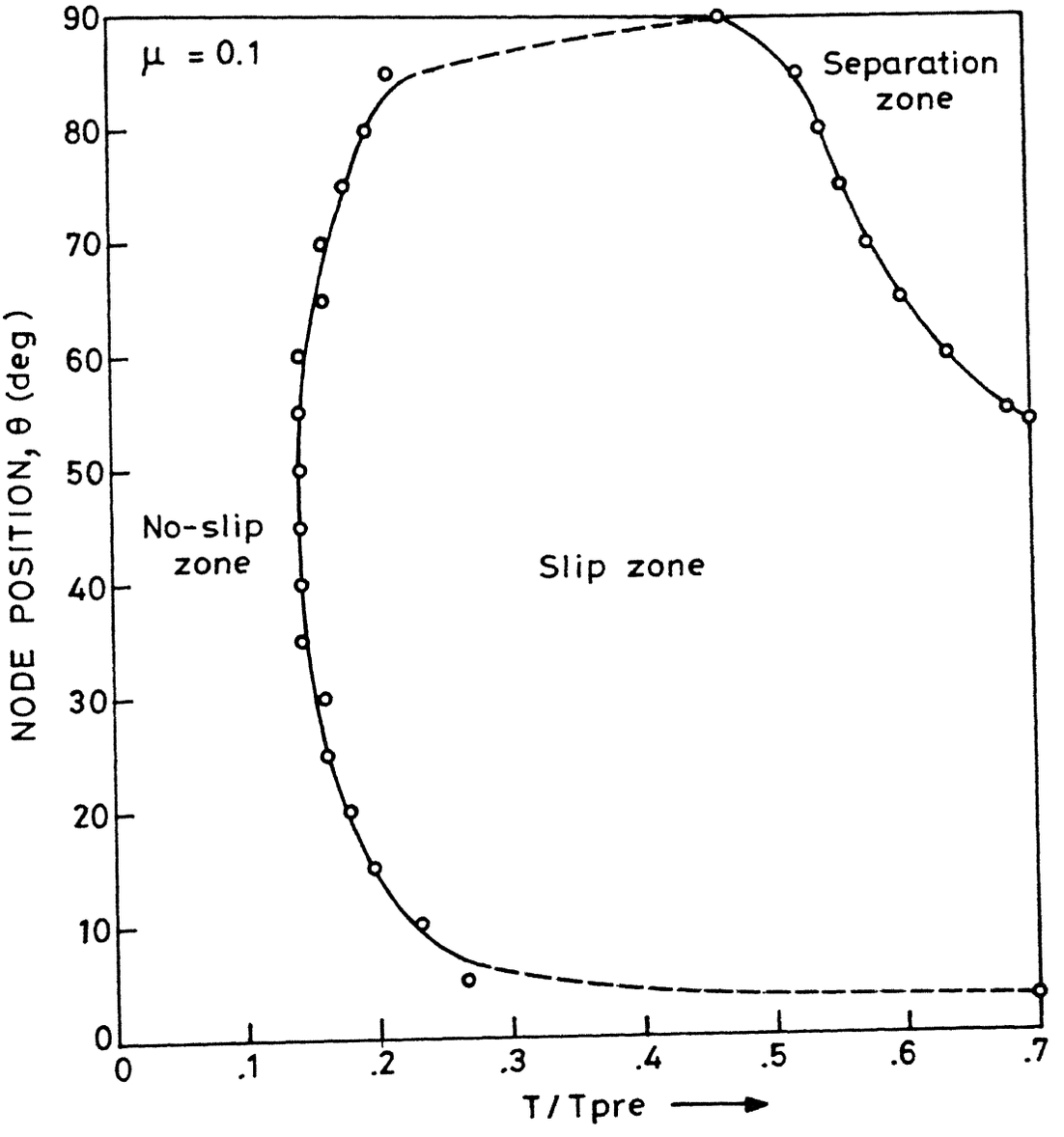


Fig. 4.3 Interface zones while loading in tension from undeformed state (using minimum dissipation of energy approach)

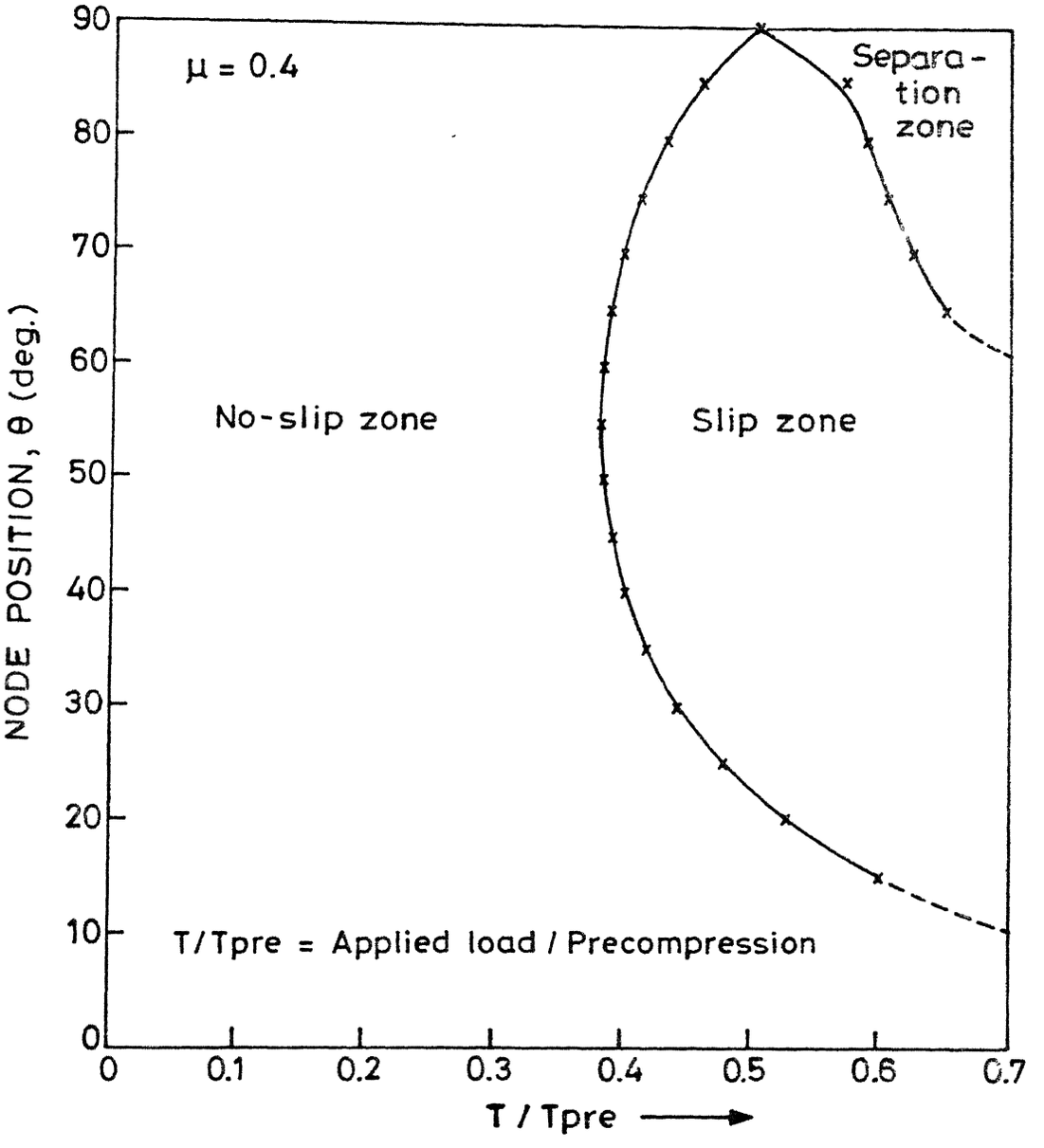


Fig.4.4 Interface zones while loading in tension from undeformed state (without minimizing energy of dissipation)

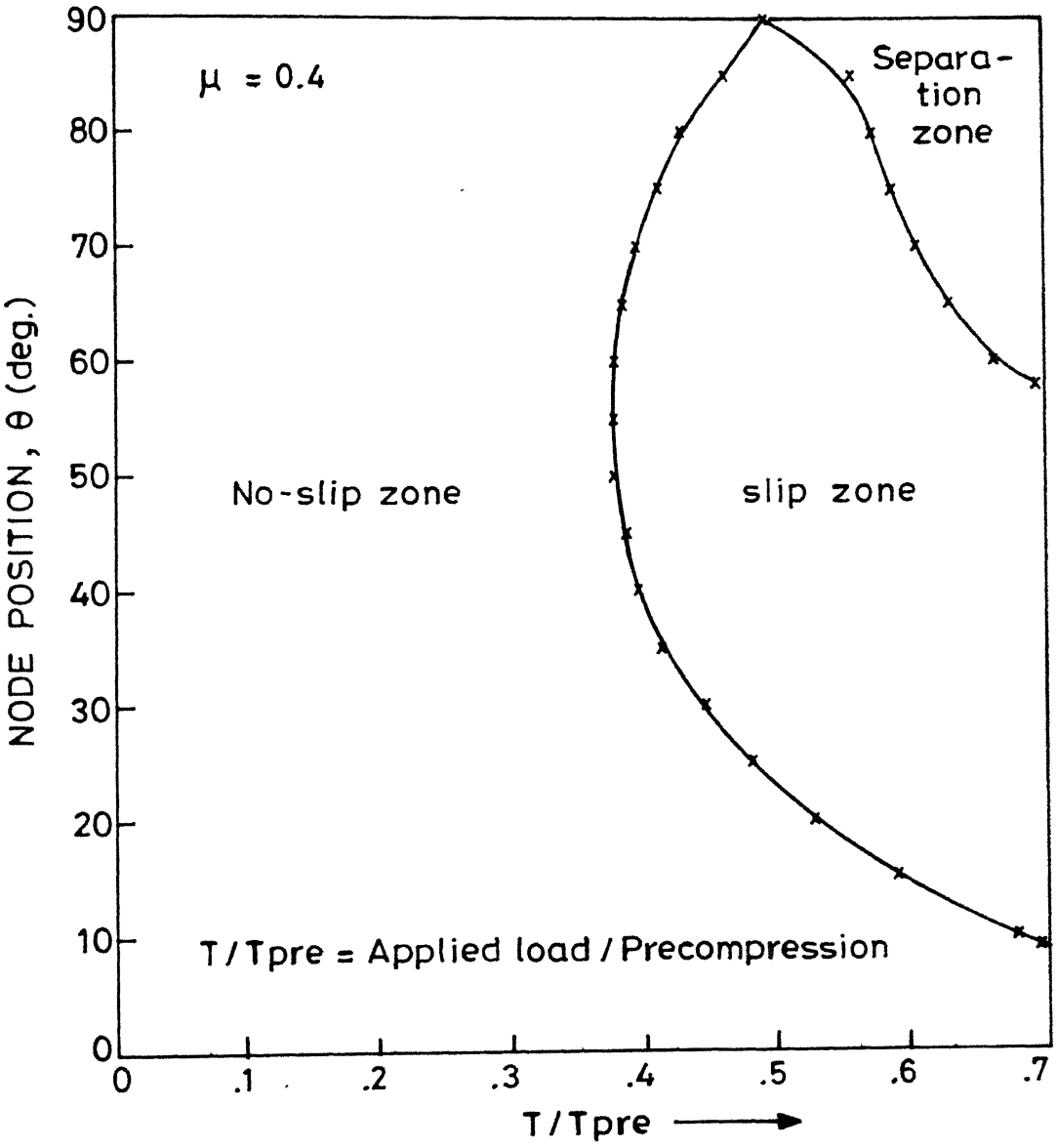


Fig. 4.5 Interface zones while loading in tension from undeformed state, for $\mu = 0.4$ (using minimum dissipation of energy approach)

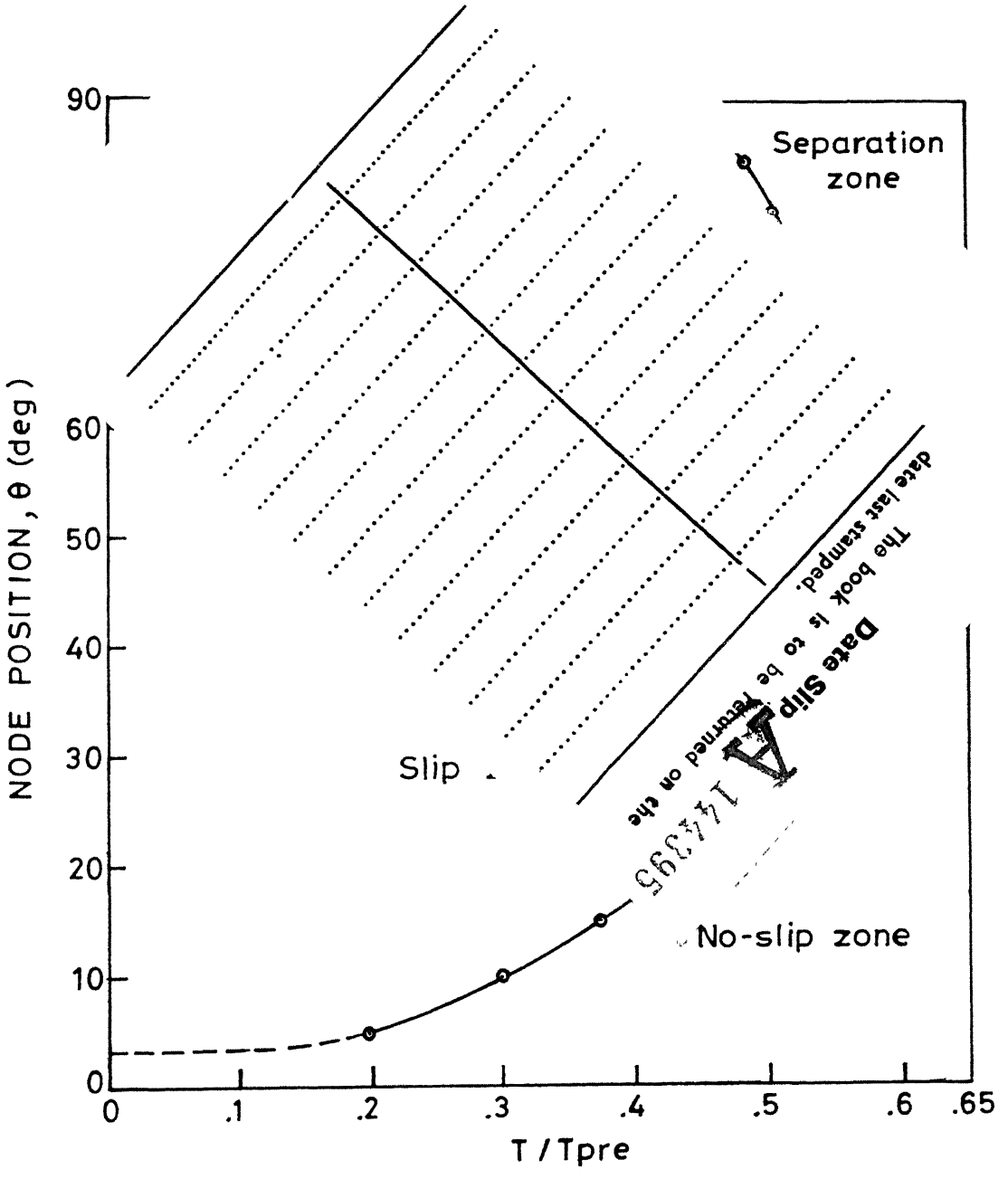


Fig.4.6 Interface zones while unloading tension.
(without minimizing energy of dissipation)

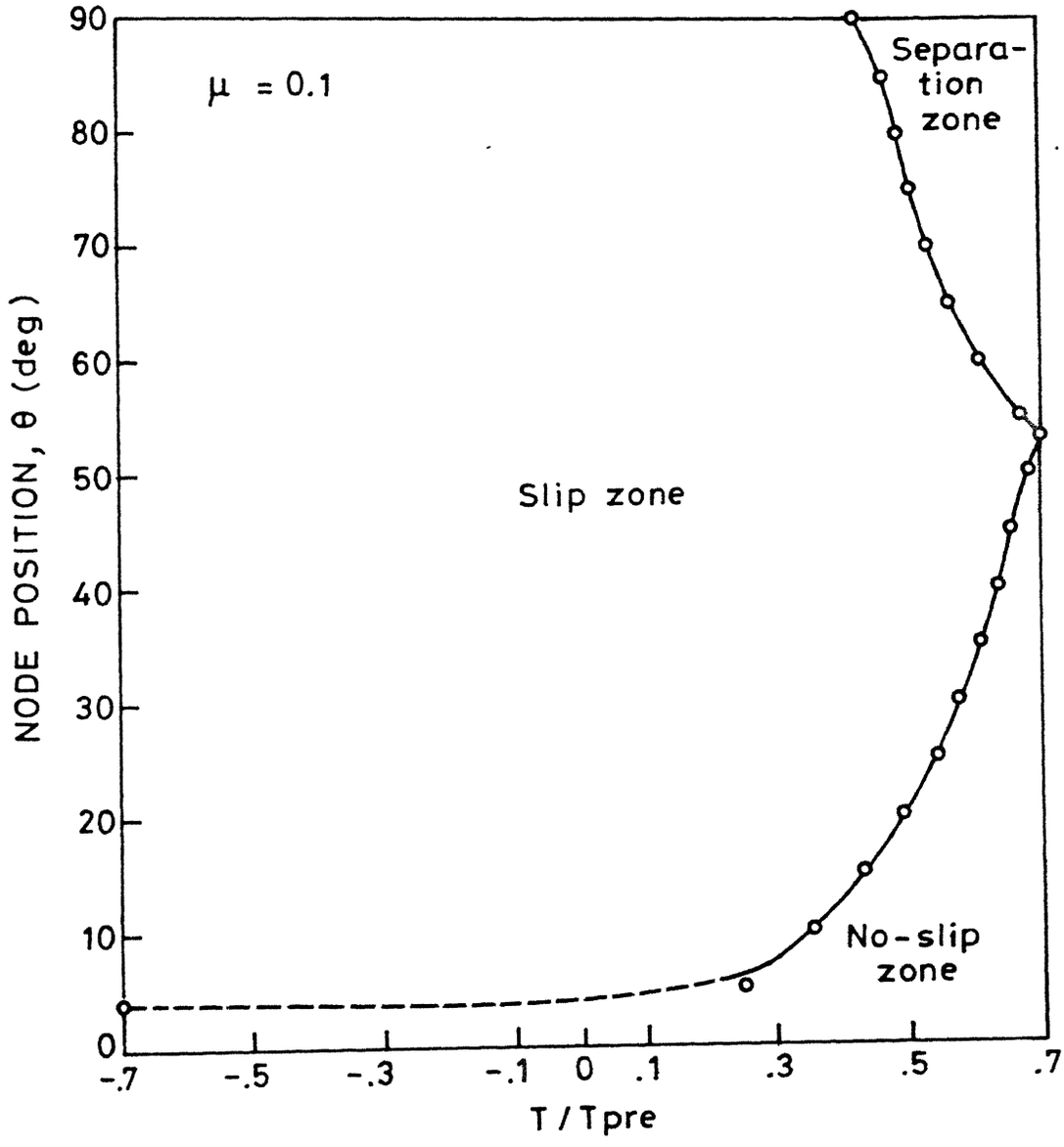


Fig. 4.7 Interface zones while unloading tension and loading in compression (using minimum dissipation of energy approach)

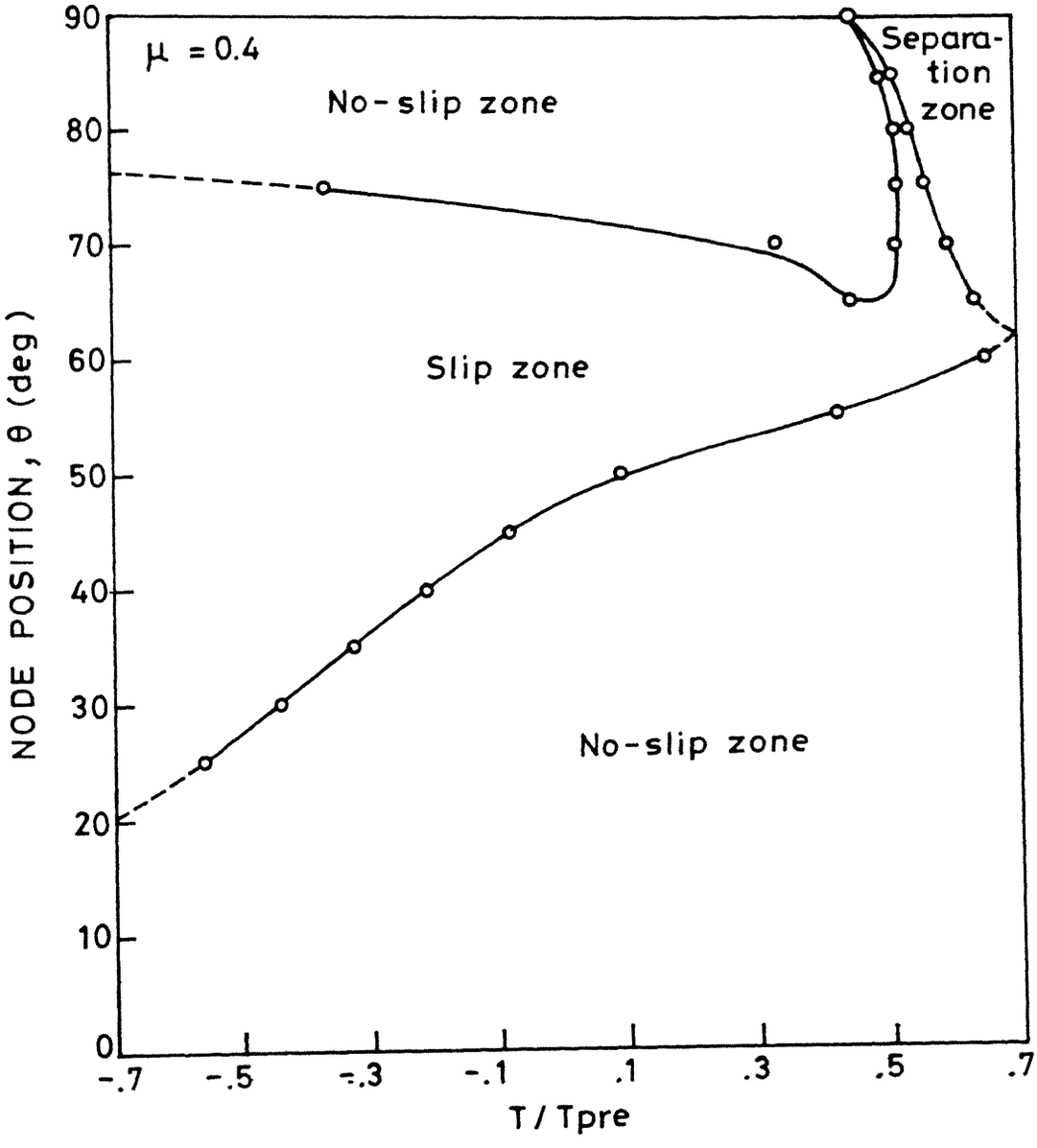


Fig.4.8 Interface zones while unloading tension and loading in compression (without minimizing energy of dissipation)

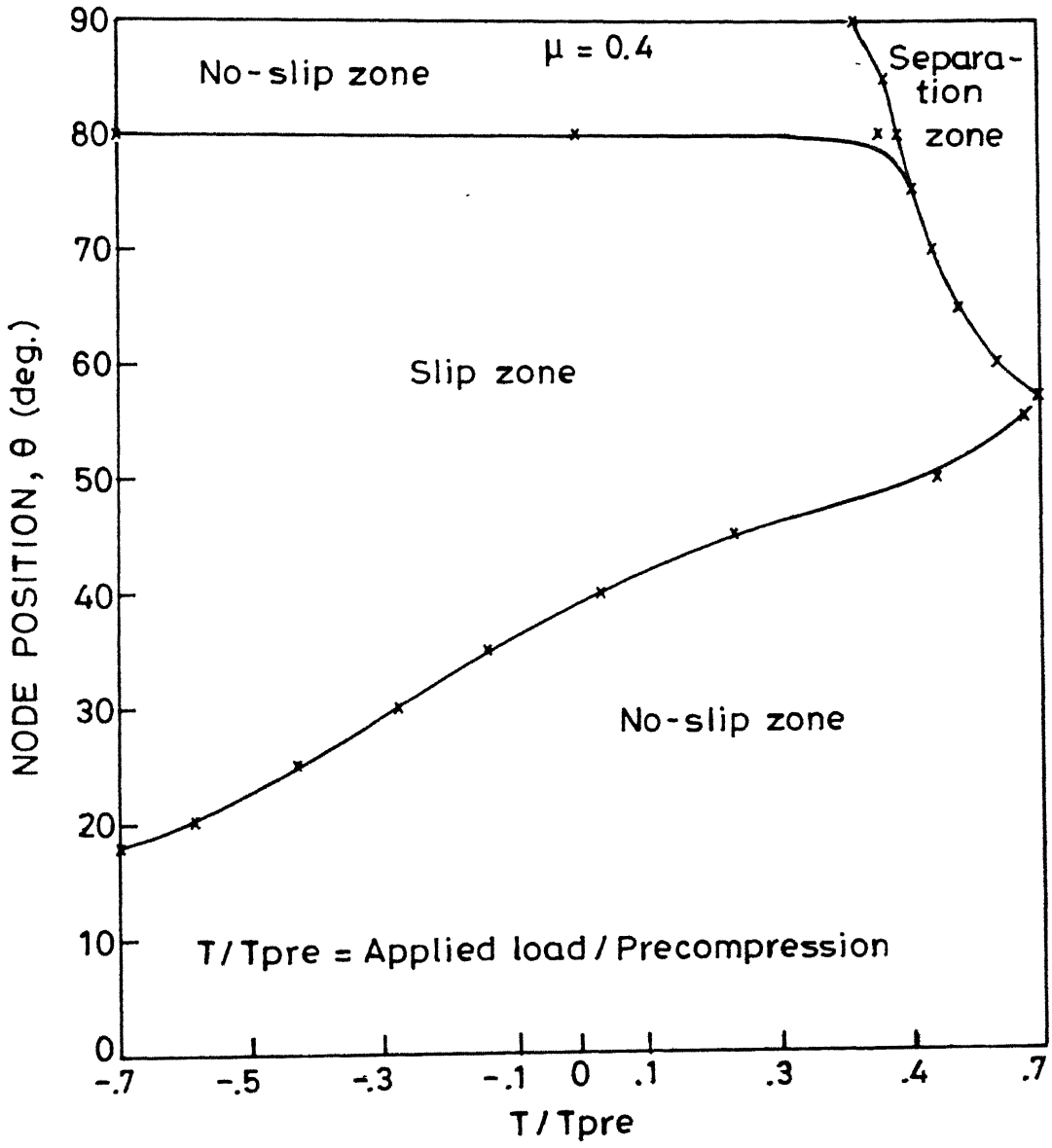


Fig.4.9 Interface zones while tension unloading and loading in compression, for $\mu = 0.4$ (using minimum dissipation of energy approach)

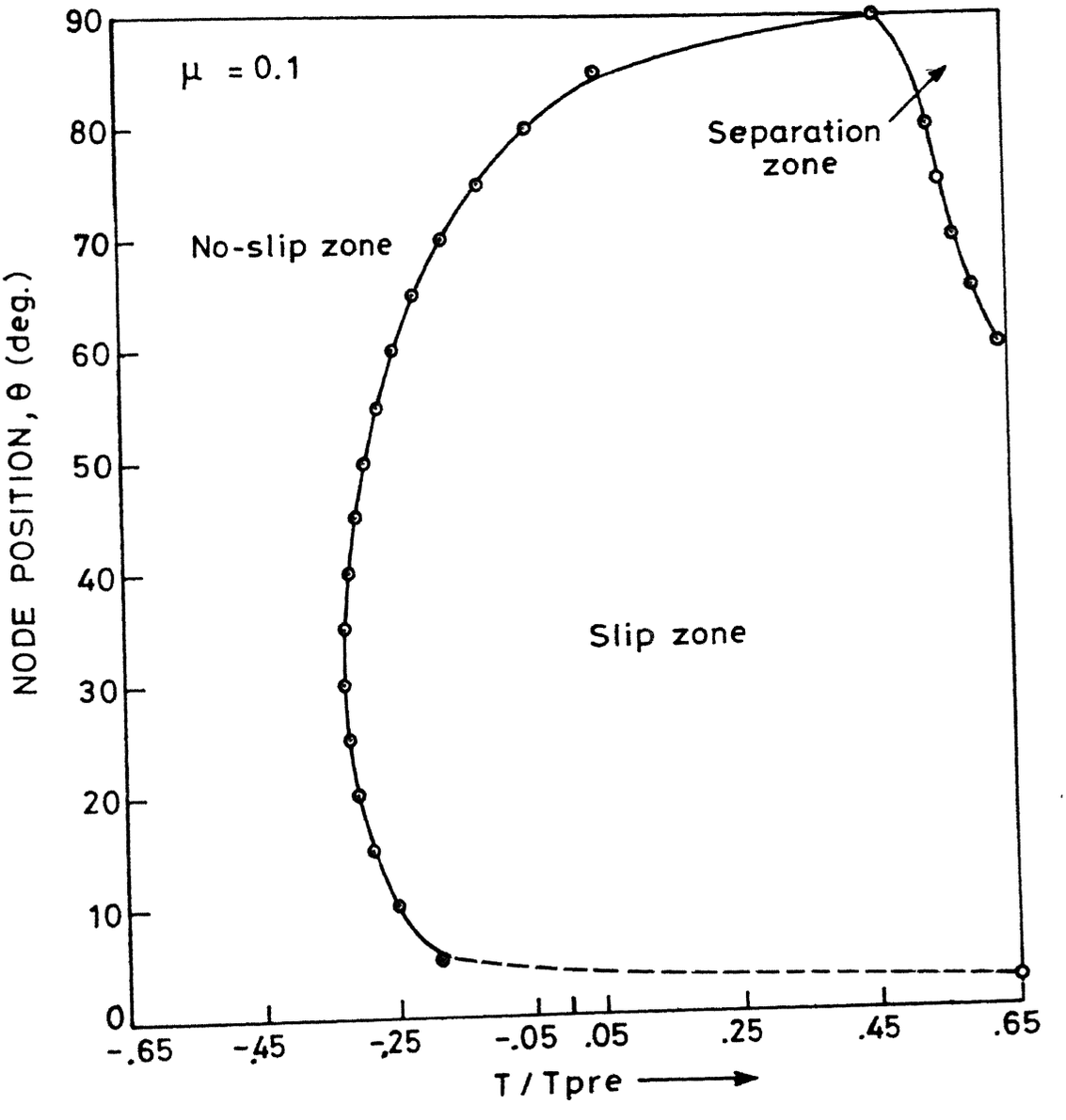


Fig.4.10 Interface zones while unloading compression and loading in tension (without minimizing energy of dissipation)

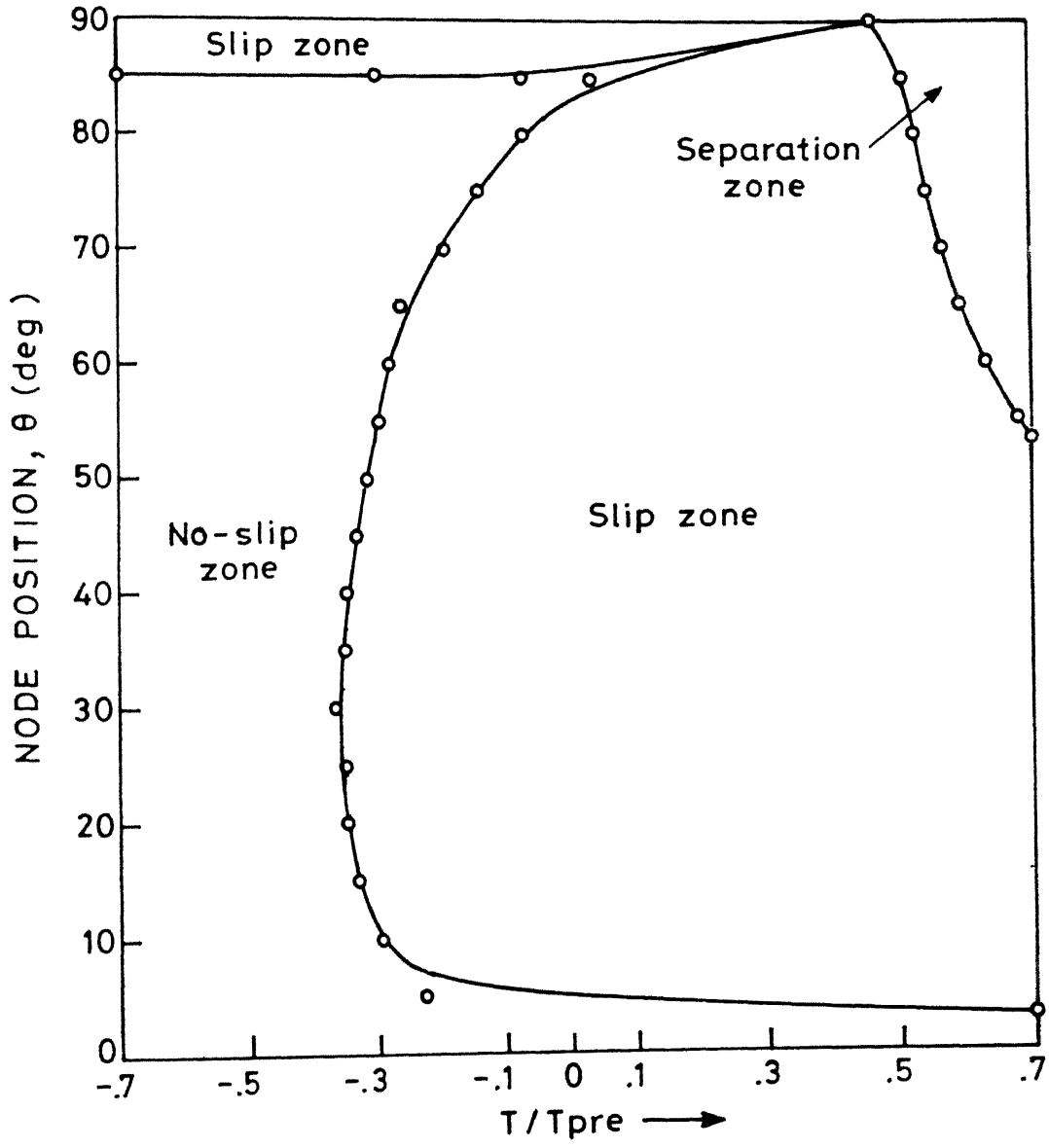


Fig. 4.11 Interface zones while unloading compression and loading in tension for $\mu = 0.1$ (using minimum dissipation of energy approach)

113079

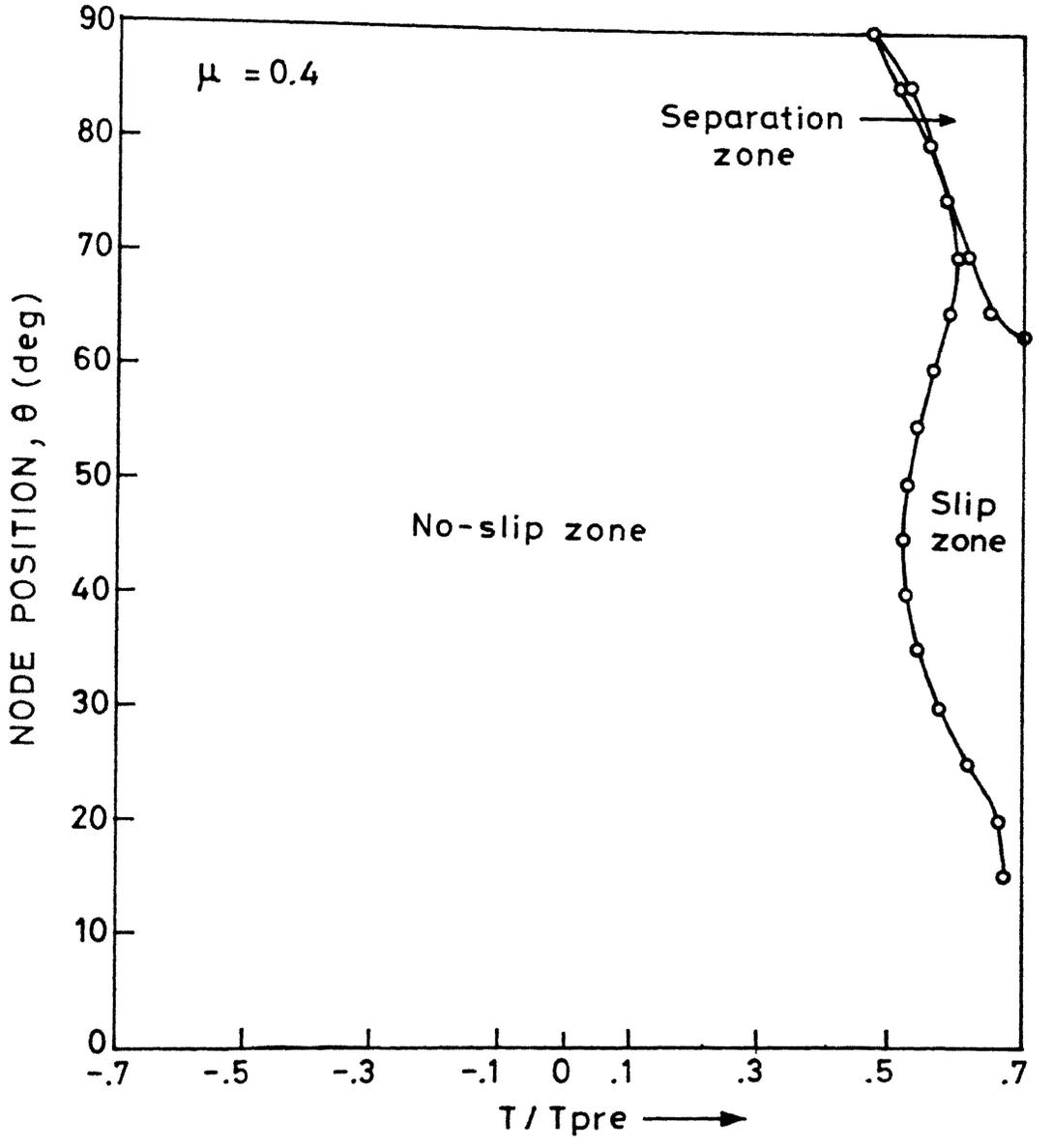


Fig.4.12 Interface zones while unloading compression and loading in tension (without minimizing energy of dissipation)

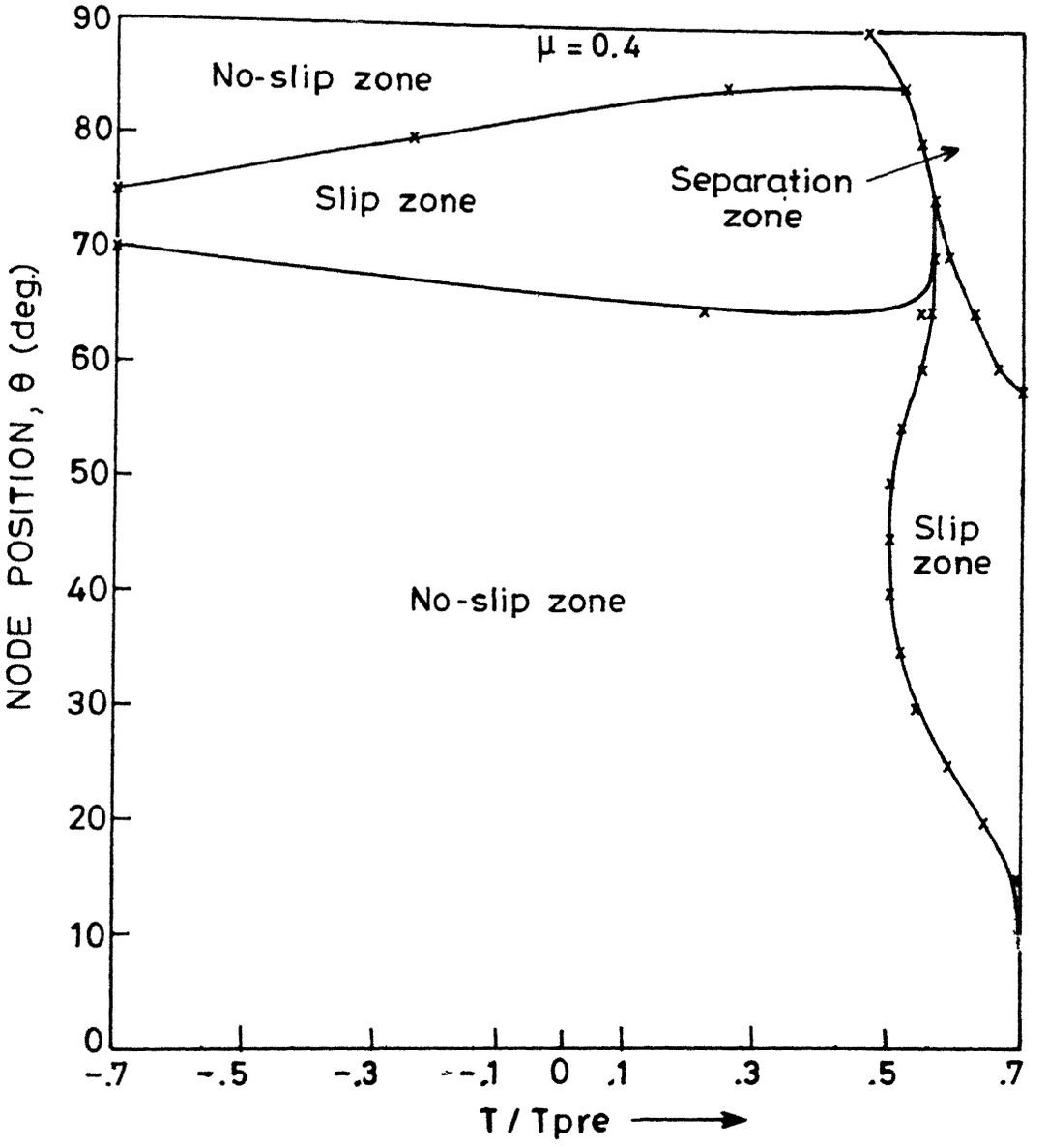


Fig. 4.13 Interface zones while compression unloading and loading in tension, $\mu = 0.4$ (using minimum dissipation of energy approach)

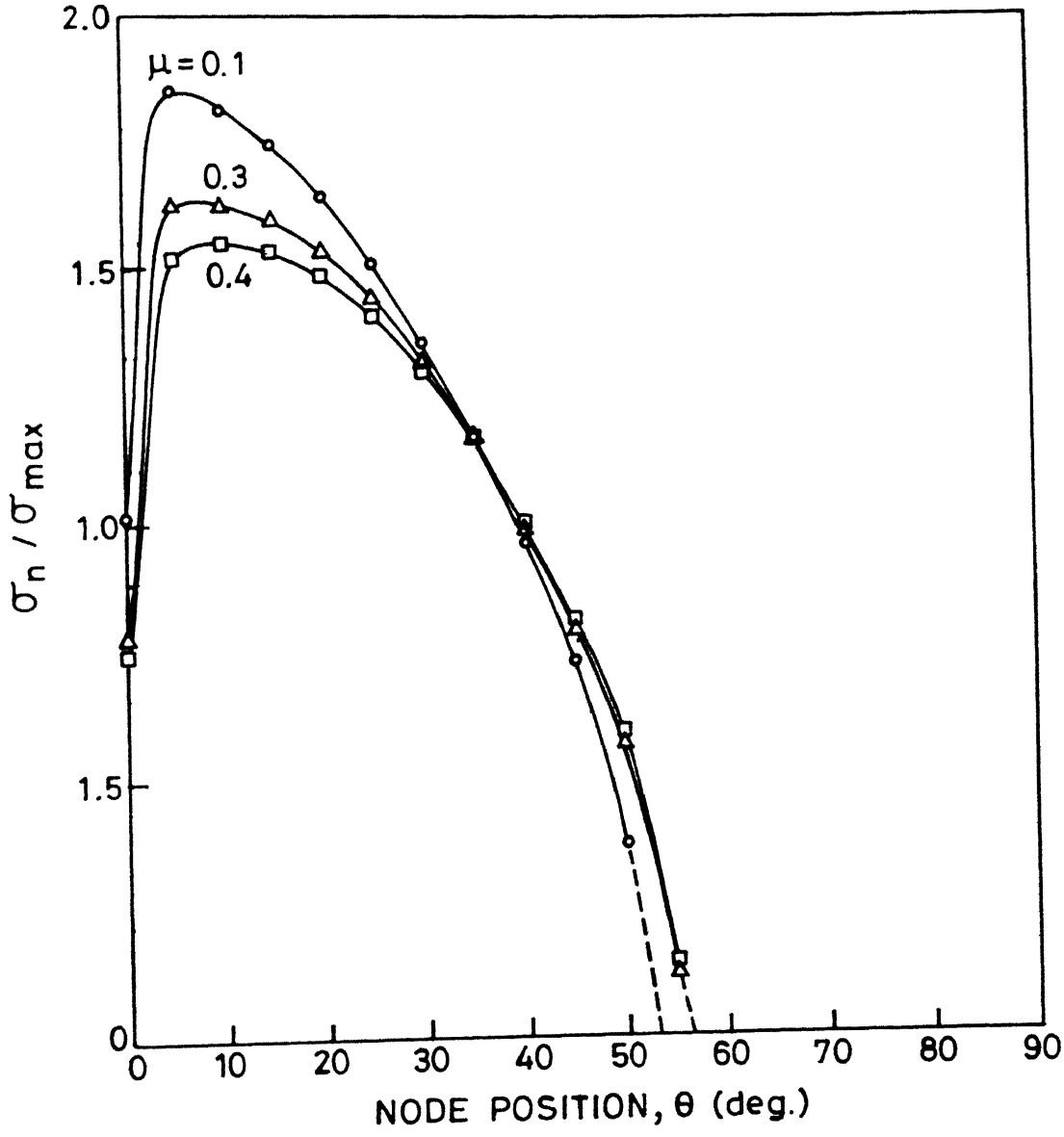


Fig.4.14 Variation of normal stress over contact length, for different μ (at maximum tensile load, T/Tpre = 0.7)

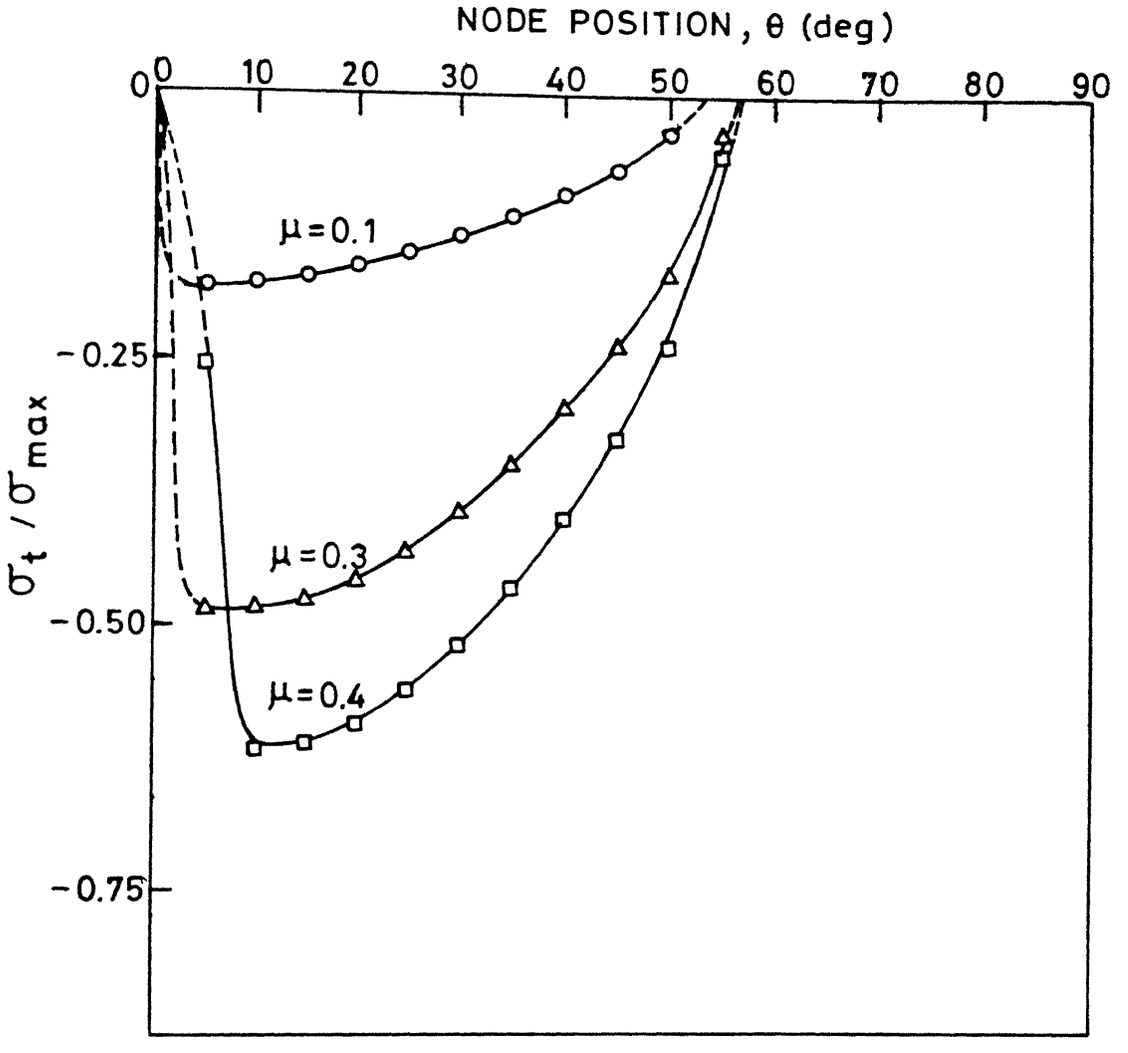


Fig.4.15 Variation of tangential stress over contact length, for different μ (at maximum tensile load, T/Tpre = 0.7)

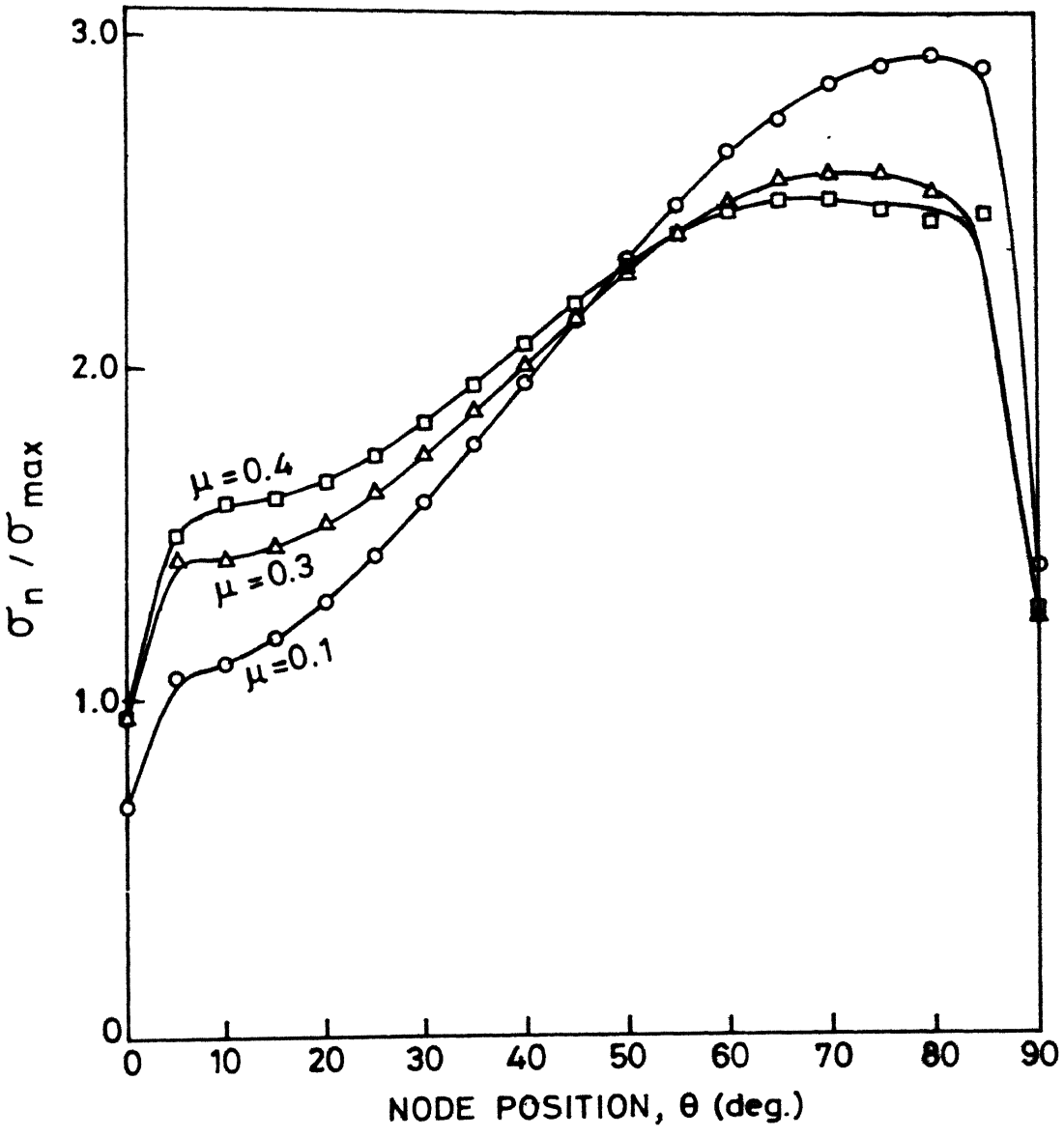


Fig.4.16 Variation of normal contact stress over contact length, at different μ (at maximum compressive load, T/Tpre = -0.7)

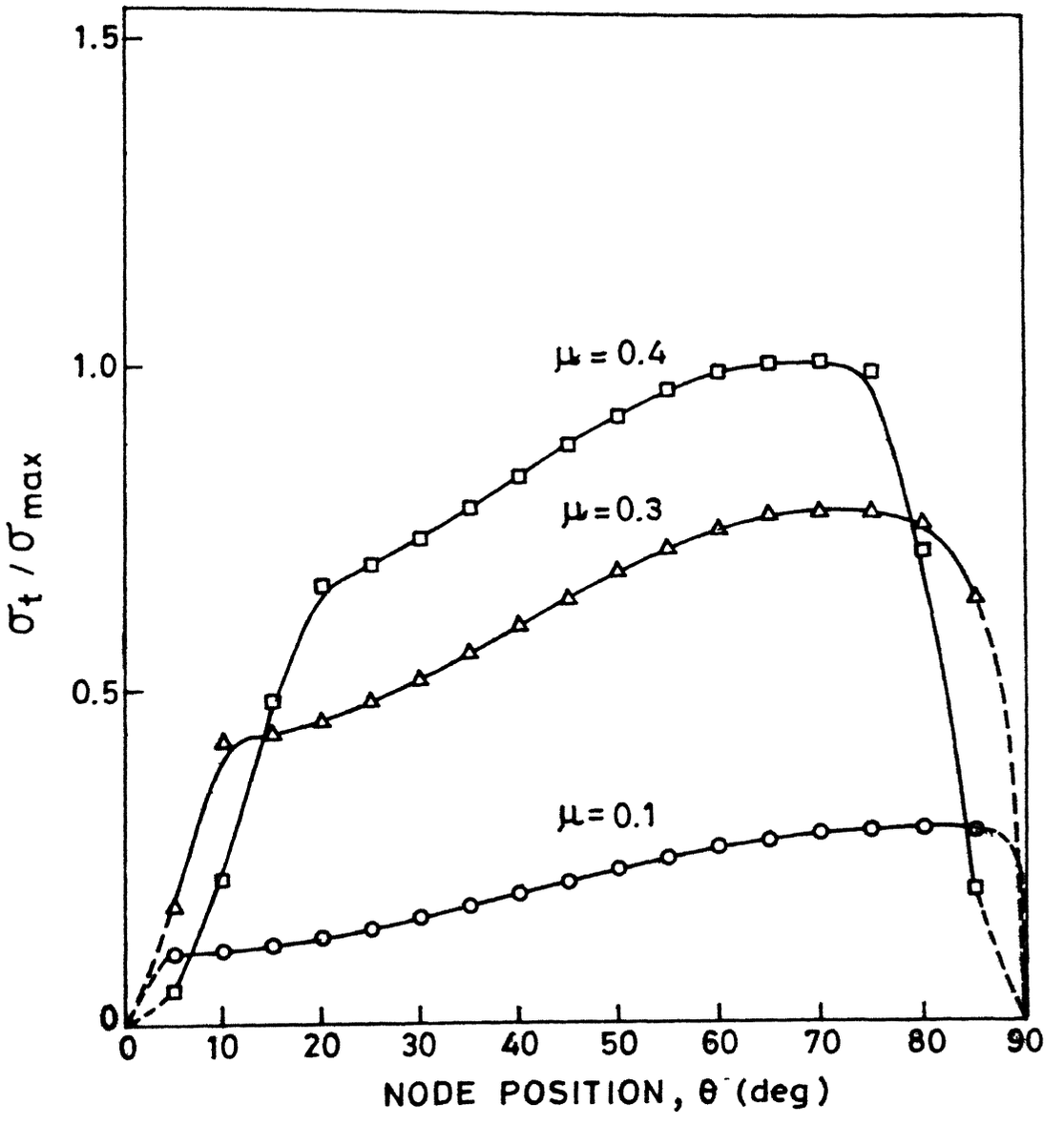


Fig.4.17 Variation of tangential stress over contact length, at different μ (at maximum compressive load, T / Tpre =-0.7)

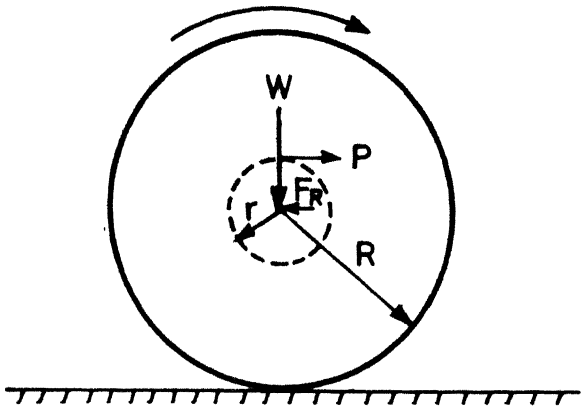


Fig.4.18(a) Cylinder rolling on rigid surface.

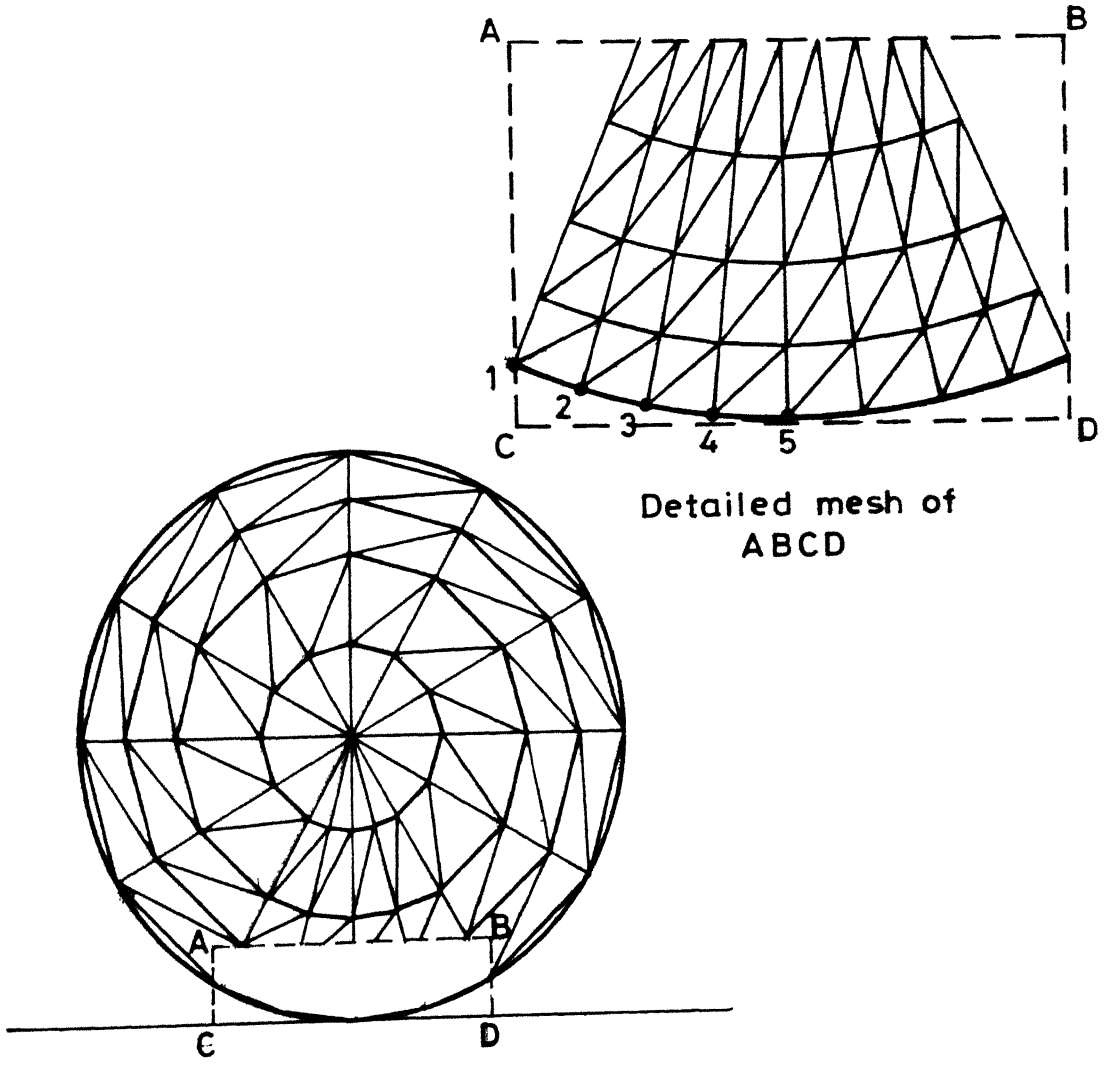


Fig.4.18 (b) Representative mesh

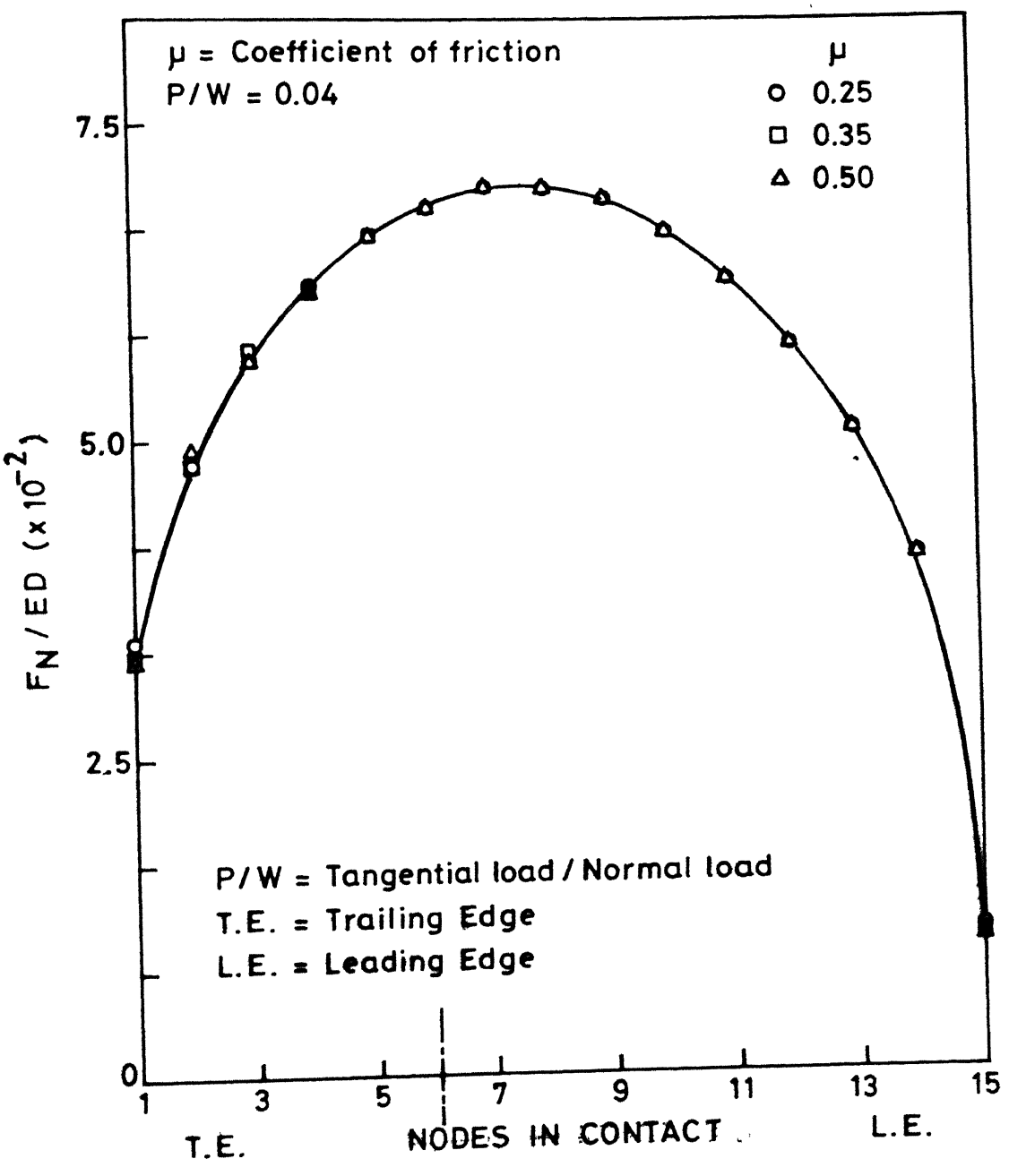


Fig.4.19 Effect of friction upon normal force distribution. (W/ED = 0.834)

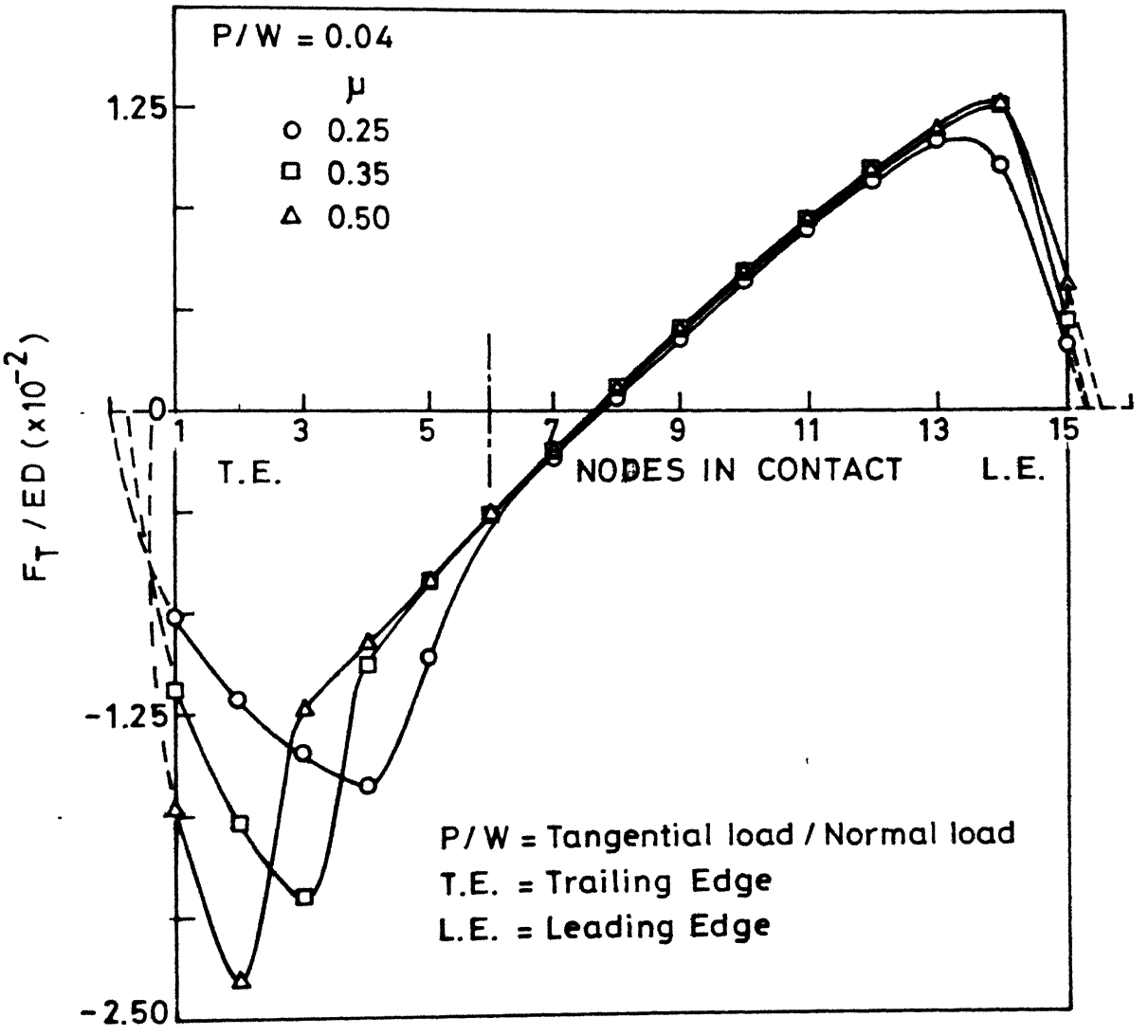


Fig. 4.20 Effect of friction upon tangential contact force distribution (W/ED = 0.834)

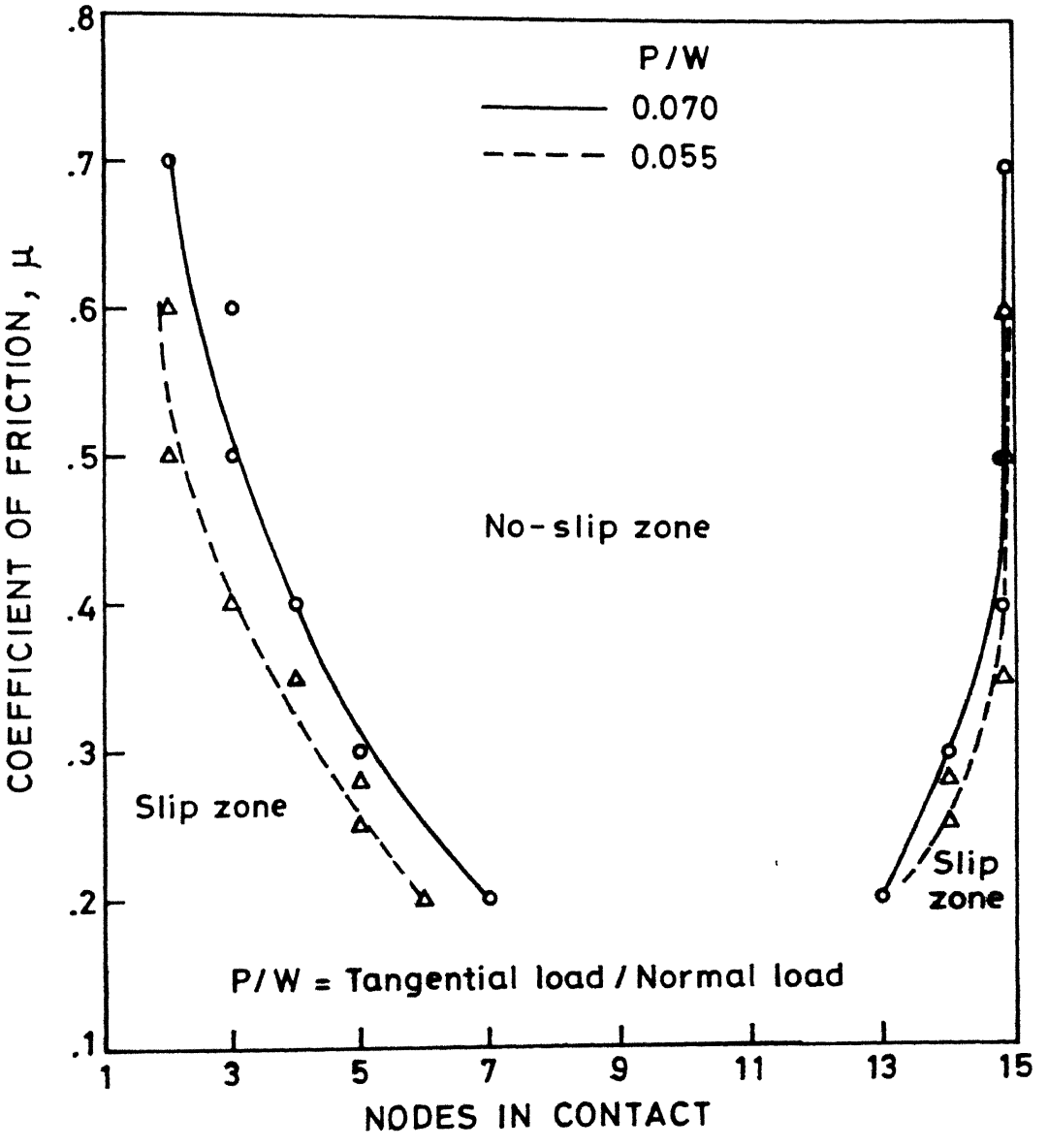


Fig.4.21 Variation of slip and no-slip zones over contact area with friction (at different P/W) (W/ED = 0.834)

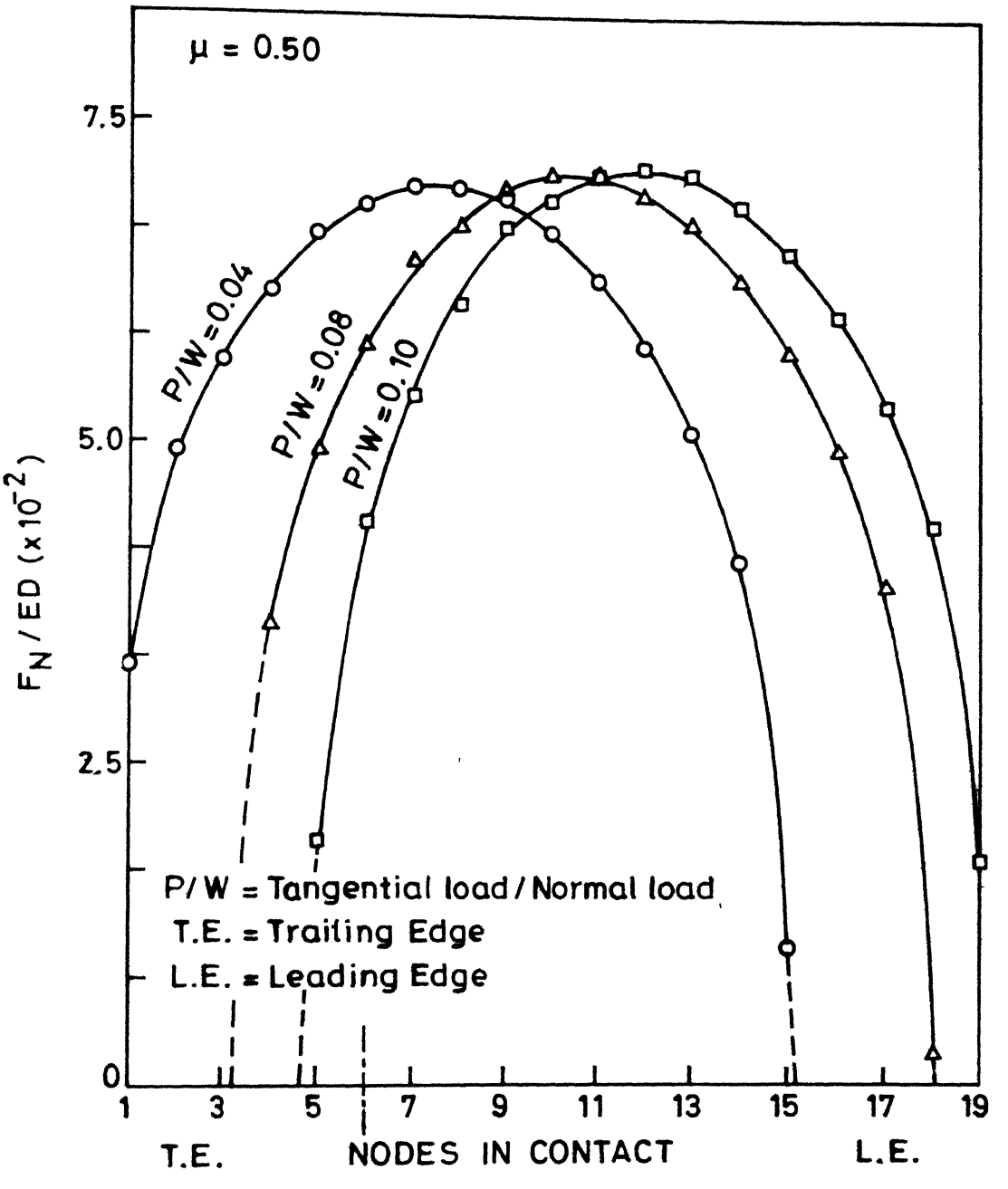


Fig.4.22 Distribution of normal force over contact length, at different P (at constant μ and W) (W/ED = 0.834)

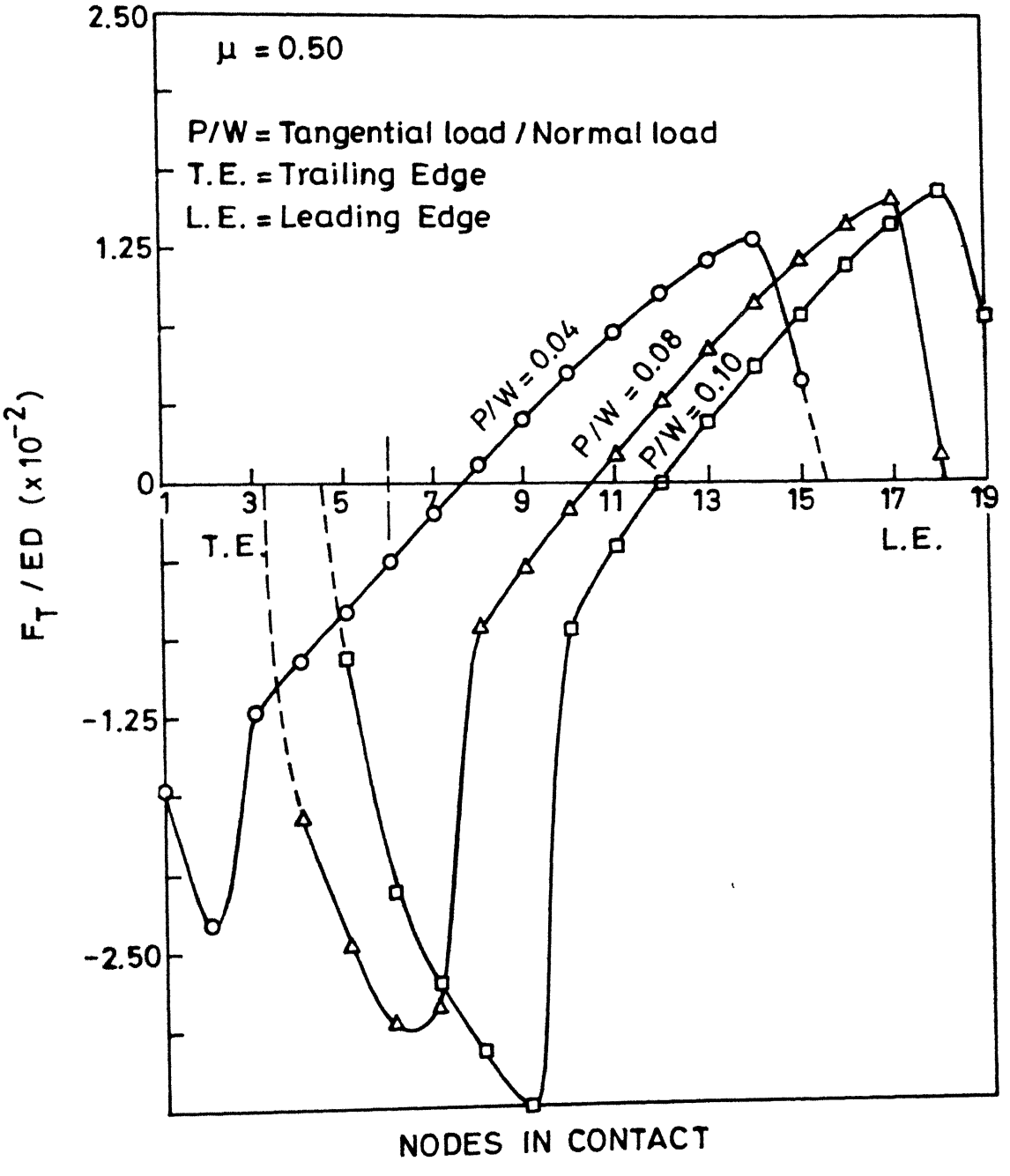


Fig.4.23 Distribution of tangential force over contact length, at different P (at constant μ and W) (W/ED = 0.834)

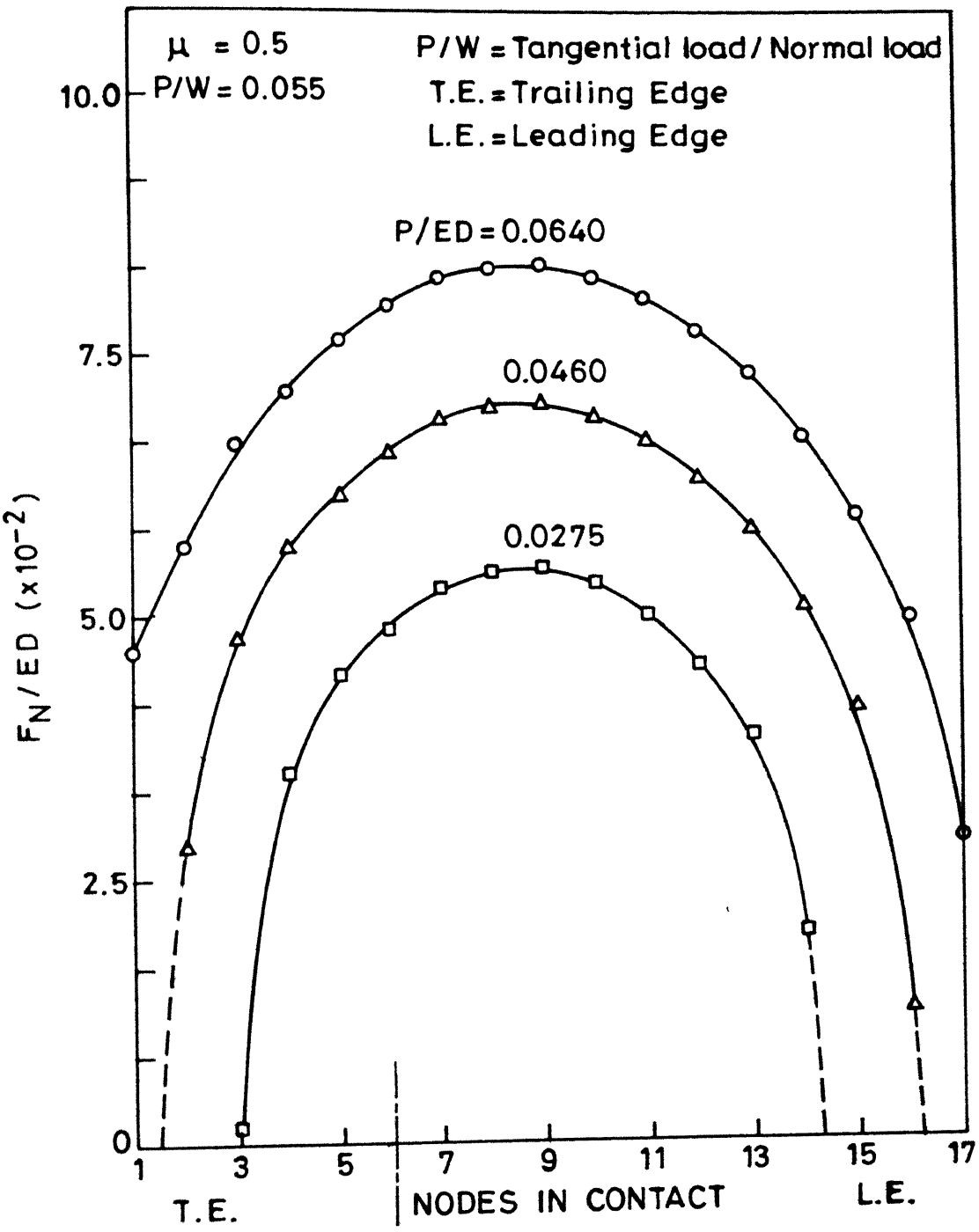


Fig.4.24 Distribution of normal contact force at constt. P/W & μ (W/ED = 0.834)

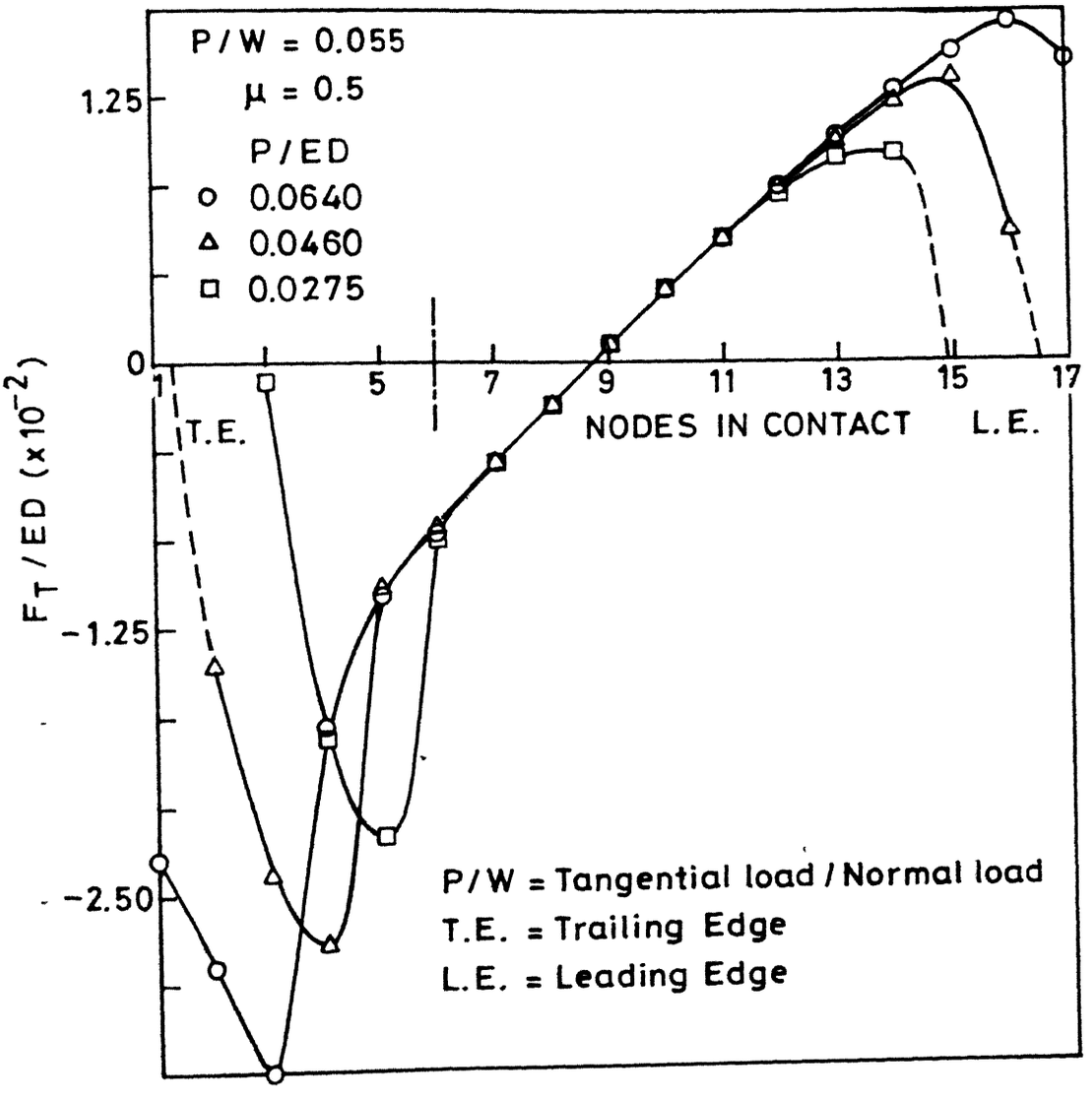


Fig.4.25 Distribution of tangential contact force at constant P/W & μ (W/ED = 0.834)

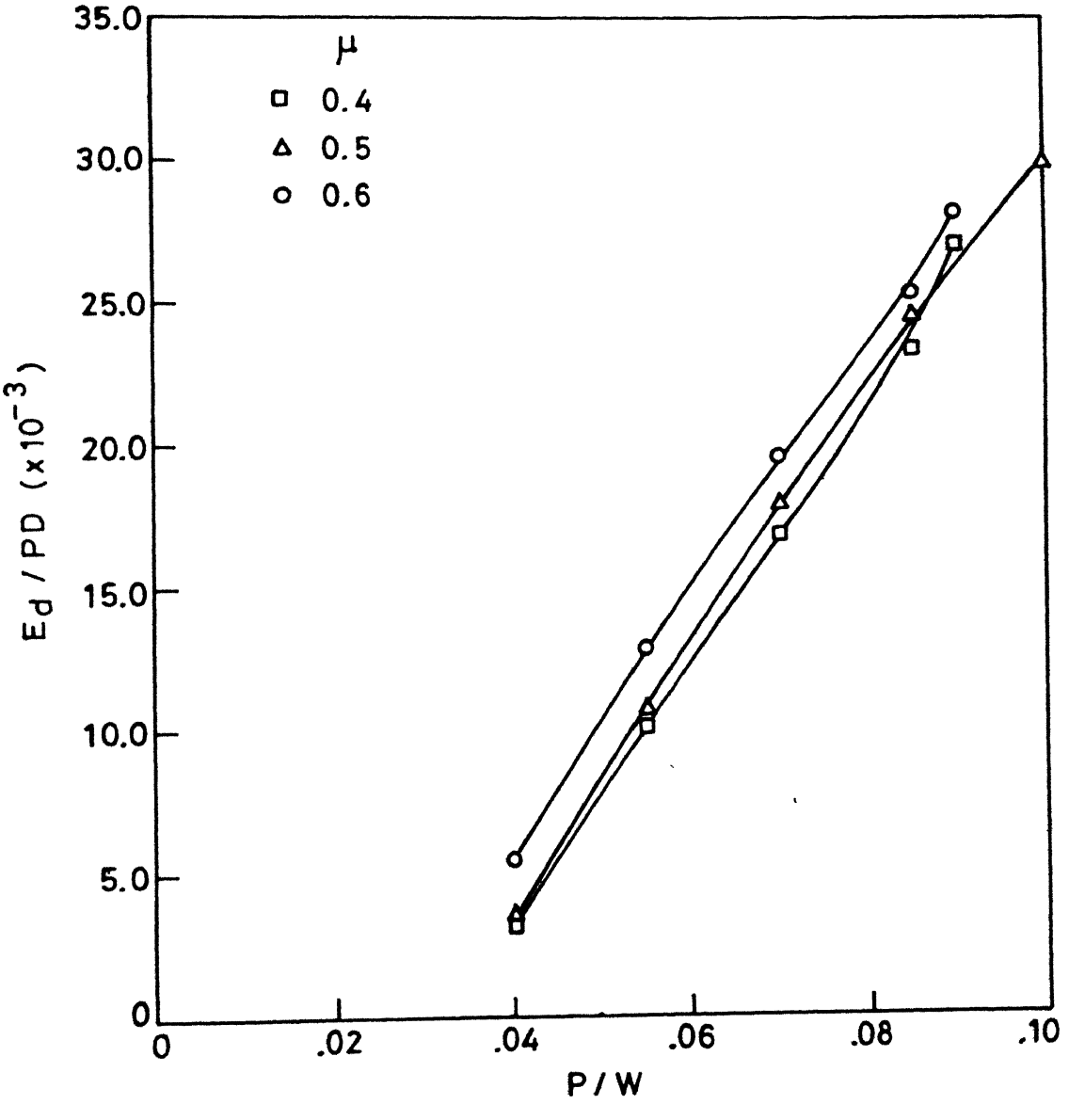


Fig.4.26 Variation of energy of dissipation (E_d) with P/W at different μ (W/ED = 0.834)

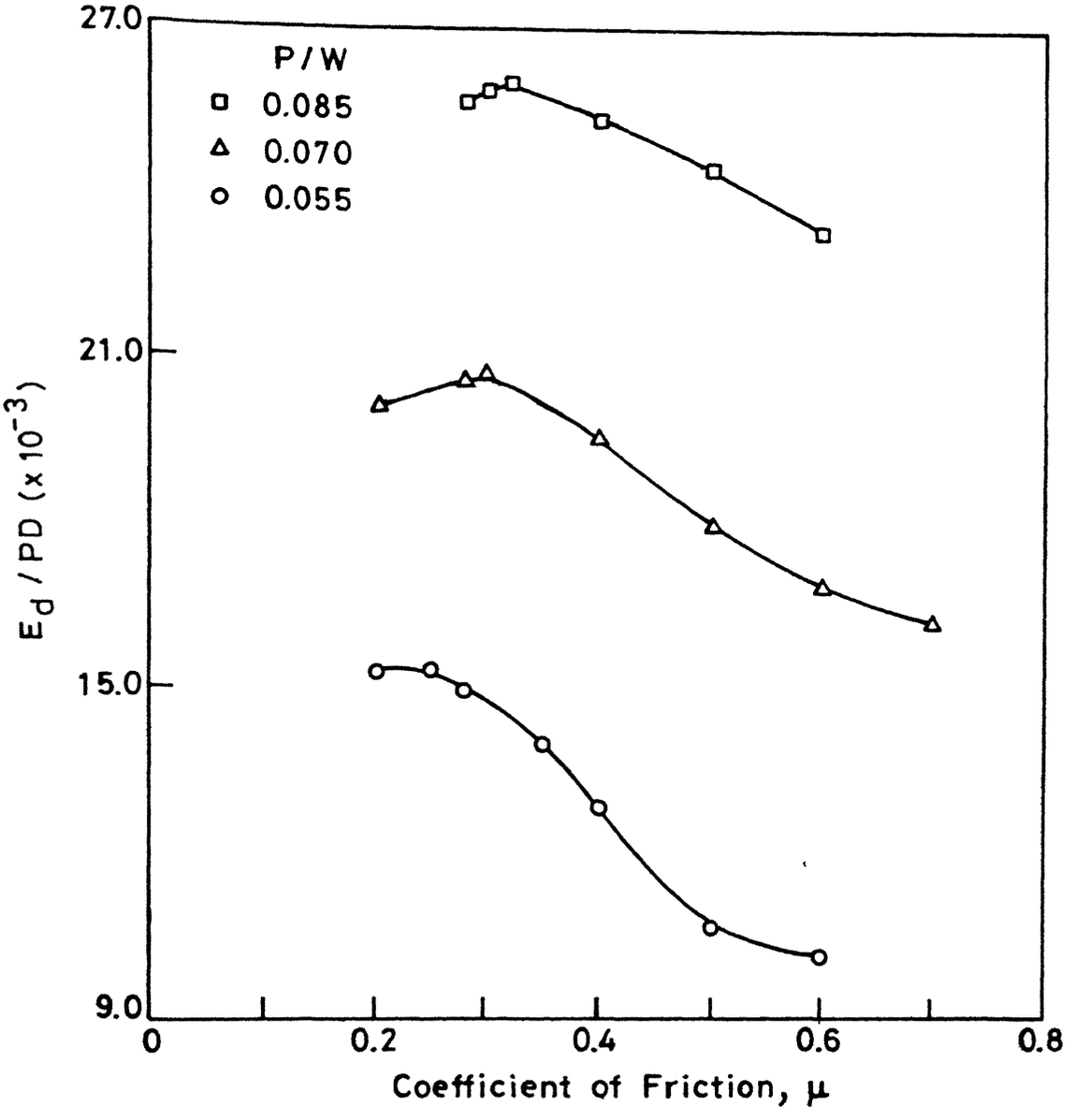


Fig.4.27 Effect of friction upon energy of dissipation (E_d) at different P/W (W/ED = 0.834)

CHAPTER V

CONCLUSIONS AND SUGGESTIONS FOR FUTURE WORK

The solutions of dynamic contact problems have been presented using the finite element and minimum dissipation of energy principle. Based upon the results presented in chapter-IV the following conclusions can be drawn :

1. Using suggested procedure it is not required to keep track of the direction of frictional resistance during the various stages of loading. The procedure itself takes care of all such situations.

2. In complex contact conditions the present method leads to more exact results with ease. For the same accuracy by the method without dissipation energy will require very fine mesh and very small load steps.

Suggestions for Future Work :

1. More accurate element can be used to make the program more efficient.

2. A more generalised rolling contact problem can be attempted wherein spin, creepage, etc. are also considered. The feasibility of employing this algorithm in solving the three dimensional rolling problems can be explored.

REFERENCES

1. Bathe K.J., "Finite Element Procedures in Engineering Analysis," Prentice-Hall, 1990

2. Bathe K.J. and Choudhary Anil, "A Solution Method for Planar and Axisymmetric Contact Problem," International Journal for Numerical Methods in Engineering, 21, 65-88, 1985

3. Chan S.K. and Tuba I.S., " A Finite Element Method for Contact Problems of Solids Bodies - Part I : Theory & Validation," Int. J. of Mech. Sc., 13, 615-625, 1971

4 . Chandrasekaran N., Haisler W.E. and Goforth R.E., "A Finite Element Solution for Contact Problems with Friction," International Journal for Numerical Methods in Engineering, 24, 477-495, 1987

5. Fellippa C.A., "Solution of Linear Equations with Skyline-Stored Symmetric Matrix," Computers & Structures, 5, 13-29, 1974

6. Francavilla A. and Zienkiewicz O.C., "A Note on Numerical Computation of Elastic Contact Problems," International Journal for Numerical Methods in Engineering, 9, 913-924, 1975

8. Fredriksson B., "Finite Element Solution of Surface Non-Linearities in Structural Mechanics with Special Emphasis to Contact and Fracture Mechanics Problems," Computers & Structures, 6, 281-290, 1976

9. Fredriksson B., Rydholm G. and Sjoboln, "Variational inequalities in the structural mechanics with emphasis on the contact problem," Proc. of Non-linear solid and structural mechanics, 863-884, Geilo, Norway, 1977

10. Gaertner R., "Investigation of Plane Elastic Contact Allowing for Friction," Computers & Structures, 7 ,59-63, 1977

11. Gladwell G.M.L., "Contact Problems in Classical theory of Elasticity," Sijthoff and Nordhoff, The Netherlands, 1973

12. Hertz H., J. of math 92,156-171, (1882) (original in German), Miscellaneous papers (in English), Macmillan, London (1896)

13 Hung D and Saxce G, "Frictionless Contact of Elastic Bodies by Finite Element Method and Mathematical Programming technique, " Computers and Structures,.11, 55-67, 1980

14. Jing H.-S. and Liao M.L., "An Improved Finite Element Scheme for Elastic Contact Problems with Friction," Computers & Structures, 35, 571-578, 1990

15. Johnson K.L., "Effect of Tangential Contact Force upon the Rolling Motion of an Elastic Sphere on a Plane," Trans ASME, Journal of Applied mechanics, 25, 1958

16 Johnson W. and Mellor P.B., Engineering Plasticity, van Nostrand Reinhold, 1973

17. Kalker J.J., "The Computation of Three Dimensional Rolling Contact with Dry Friction" Int. J. for Num. in Engg., Vol 14, 1293-13Ø7, 1979

18. Kishore N.N., Ph.D. Thesis, I.I.T. Kanpur, 1979

19. Kishore P.V., "Solution Method to Contact Problems-using minimum dissipation of energy approach," M.Tech. Thesis, I.I.T. Kanpur, 1988

2Ø. Kuester J.L. and Mize J.H., Optimization Techniques with Fortran, McGraw Hill Book Co., 1973

21. Liu C. and Paul B., "Rolling Contact with Friction and Non-Hertzian Pressure Distribution," (Trans. of ASME), J. of Appl. Mech. 56, 814-2Ø, 1989

22. Moore D.F.,The Friction of Pneumatic Tyres, Elservier Scientific Pub. Co. (1975).

23. Muskhelishville N.I., "Some Basic Problems of the Mathematical theory of Elasticity," Sijthoff and Nordhoff, The Netherlands,1963

24. Oden AND Pires, "Non-Local and Non-linear Friction laws and Variational Principles for Contact Problems in Elasticity," J. Applied Mech. 5Ø(1), 67-76, 1983

25. Okamoto N. and Nakazawa M., "Finite Element Incremental Contact Analysis with various Frictional Conditions," International Journal for Numerical Methods in Engineering 14, 337-357, 1979

26. Ohte S.," Finite Element Analysis of Elastic Contact Problems," Bulletin of JSME, 16, 797-8Ø4, 1973

27 Poritsky H., " Stress and Deflections of Cylindrical Bodies in Contact," Trans ASME Jr of Applied Mechanics, 18, 191, 195Ø

28. Padovan J., Tovichakchaikul and Zeid I., "Finite Element Analysis of Steadily Moving Contact Fields," Computers and structures 18, 191-2ØØ, 1984

29. Rahman M.U., Rowlands R.E. and Cook R.D., "An Iterative Procedure for Finite Element Stress Analysis of Frictional Contact Problems," Computers & Structures 18, 947-954, 1984

3Ø. Rao S.S., Optimization Theory and Application, Wiley Eastern Ltd., 2nd Ed. , 199Ø

31. Sachdeva T.D. and Ramakrishnan C.V., "A Finite Element

Solution for the Two-Dimensional Elastic Contact Problems with Friction," International Journal for Numerical Methods in Engineering 17, 1257-1271,1981

32. Timoshenko S.P. & Goodier J.N., Theory of Elasticity McGraw Hill Book Co., 3rd Ed., 1982

33. Torstenfelt Bo, "Contact Problems with Friction in General Purpose Finite Element Computer Program," Computers and Structures, 16, 487-493, 1983

34. Wilson and Parsons, " Finite element analysis of contact problems using differential displacements," Computers and Structures, 2, 387-395, 197Ø

35. Zeid I and Padovan J., "Finite Element Modelling of Rolling Contact," Computers & Structures 14, 163-17Ø, 1981.

36. Zochowski, A. & Myslinski A., "Rolling Contact Problems using Quasi-static Variational Formulation," Computers and Structures 4Ø,12161-1266, 1991.

APPENDIX A

SUB-STRUCTURING

The equilibrium equation

$$[\ K\]\ \{\ U\ \} = \{\ F\ \}$$

is re-arranged as shown

$$\begin{bmatrix} [K_1] & [K_2] & [K_3] \\ [K_2]^T & [K_4] & [K_5] \\ [K_3]^T & [K_5]^T & [K_6] \end{bmatrix} \begin{Bmatrix} \{U_1\} \\ \{U_2\} \\ \{U_3\} \end{Bmatrix} = \begin{Bmatrix} \{F_1\} \\ \{F_2\} \\ \{F_3\} \end{Bmatrix}$$

where,

U_1 are pescribed displacements degrees of freedom (dof)

U_2 are displacement dof corresponding to free nodes

U_3 are contact dof and prescribed force dof

Since $\{U_1\}$ is known, the equation reduces to

$$\begin{bmatrix} [K_4] & [K_5] \\ [K_5]^T & [K_6] \end{bmatrix} \begin{Bmatrix} \{U_2\} \\ \{U_3\} \end{Bmatrix} = \begin{Bmatrix} \{F_2\} \\ \{F_3\} \end{Bmatrix} + \begin{Bmatrix} \{F_{21}\} \\ \{F_{31}\} \end{Bmatrix}$$

where

$$\{F_{21}\} = -[K_2]^T . \{U_1\}$$

$$\{F_{31}\} = -[K_3]^T . \{U_1\}$$

Since $\{F_2\}$ corresponds to the internal dof, so

$$\{F_2\} = \{\emptyset\}$$

By solving the equations for U_3

$$[K_7]\ \{U_3\} = \{F_3\} + \{F_4\}$$

where

$$[K_7] = [K_6] - [K_5]^T \ [K_4]^{-1}[K_5]$$

$$\{F_4\} = \{F_{31}\} - [K_5]^T[K_4]^{-1}\{F_{21}\}$$

The evaluation of $[K_7]$ and $\{F_4\}$ can be done in preparation stage. In the evaluation of these matrices no explicit inversion is done. Back substitution with previous factorized matrices is done to compute products like $([K_4]^{-1}[K_5])$. $[K_1]$, $[K_2]$,...,$[K_6]$ are not stored separately but are obtained procedurally from the skyline stored stiffness matrix. $[K_7]$ is stored in full storage mode. All the conditions on displacements $\{U_3\}$ are applied on $[K_7]$. After solving for $\{U_3\}$, $\{U_2\}$ dof can also be obtained by substituting for $\{U_3\}$ in appropriate equation.

APPENDIX B

IMPOSITION OF CONTACT BOUNDARY CONDITIONS

The condtions of slip and no-slip over the contact region, as mentioned in section 3.2, are reproduced here for convenience.

For stick or no-slip:

$$u_{n1} = \delta_1$$

$$u_{t1} = \emptyset$$

For slip:

$$u_{n2} = \delta_2$$

$$F_{t2} = \pm \mu \, |F_{n2}|$$

subscript 1,2 corresponds to nodes. These conditions are put in the condensed stiffness matrix. Their imposition on the matrix is explained by an example given below as:

Let consider a condensed stiffness matrix $[K_c]$ for the dof corresponding to two nodes, one sticking and other slipping. The equation is given as :

$$[K_c] \{ U \} = \{ F \}$$

where

$$[K_c] = \begin{bmatrix} a_1 & b_1 & c_1 & d_1 \\ a_2 & b_2 & c_2 & d_2 \\ a_3 & b_3 & c_3 & d_3 \\ a_4 & b_4 & c_4 & d_4 \end{bmatrix}$$

$\{ U \}$ is nodal displacement vector and $\{ F \}$ is nodal force vector.

Let, the first two dof corresponds to sticking node and remaining two to slipping one. The $[K_c]$ is modified while imposing the above conditions. To apply the friction condition at the slipping node, the μ times 4^{th} row is added to the 3^{rd} row, making right hand side zero. The sign of μ is chosen such that F_t opposes u_t. The displacement conditions are imposed as shown:

$$\begin{bmatrix} 1 & \emptyset & \emptyset & \emptyset \\ \emptyset & 1 & \emptyset & \emptyset \\ a_3+\mu a_4 & b_3+\mu b_4 & c_3+\mu c_4 & d_3+\mu d_4 \\ \emptyset & \emptyset & \emptyset & 1 \end{bmatrix} \begin{Bmatrix} u_{i1} \\ u_{n1} \\ u_{i2} \\ u_{n2} \end{Bmatrix} = \begin{Bmatrix} \emptyset \\ \delta_1 \\ \emptyset \\ \delta_2 \end{Bmatrix}$$

The above equation now can be solved for displacements.